Recent results of light (anti-)(hyper-)nuclei production with ALICE at the LHC

ESTHER BARTSCH
GOETHE UNIVERSITY FRANKFURT

EMMI PHYSICS DAY 2019

Outline

- Introduction
- d, t and ^{3}He production in pp and p-Pb
- d, t, ^{3}He and ^{4}He production in Pb-Pb
- Radial and elliptic flow in Pb-Pb
- Coalescence parameters B_2 and B_3
- Evolution of d/p, t/p, ^{3}He/p ratios with multiplicity
- New results on hypertriton lifetime

Introduction – nuclear matter production

- Light (anti-)nuclei are abundantly produced at the LHC in pp, p-Pb and Pb-Pb collisions
- However, the production mechanism in high-energy physics is still not completely clear
- At high energies and densities a Quark-Gluon Plasma (QGP) is created that expands and cools down
  → Chemical freeze-out temperature T_{ch} (~150 MeV): Particle yields are fixed
  → Kinetic freeze-out temperature T_{kin} (~100 MeV): Particle momentum spectra are fixed

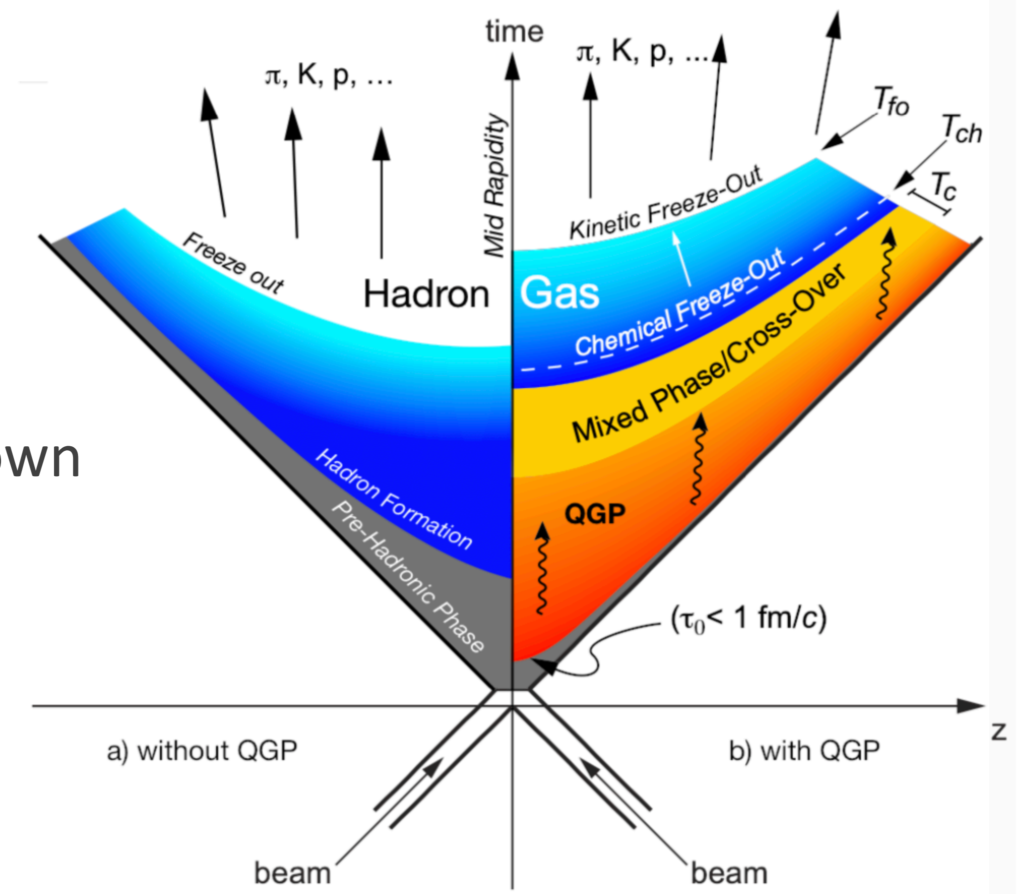

Introduction – nuclear matter production

- Two classes of models on the market to describe nuclei production:
  - → Statistical hadronization model
    - T_{ch} relevant
    - production scales with particle mass
  - → Coalescence model
    - T_{kin} relevant
    - production scales with particle radius

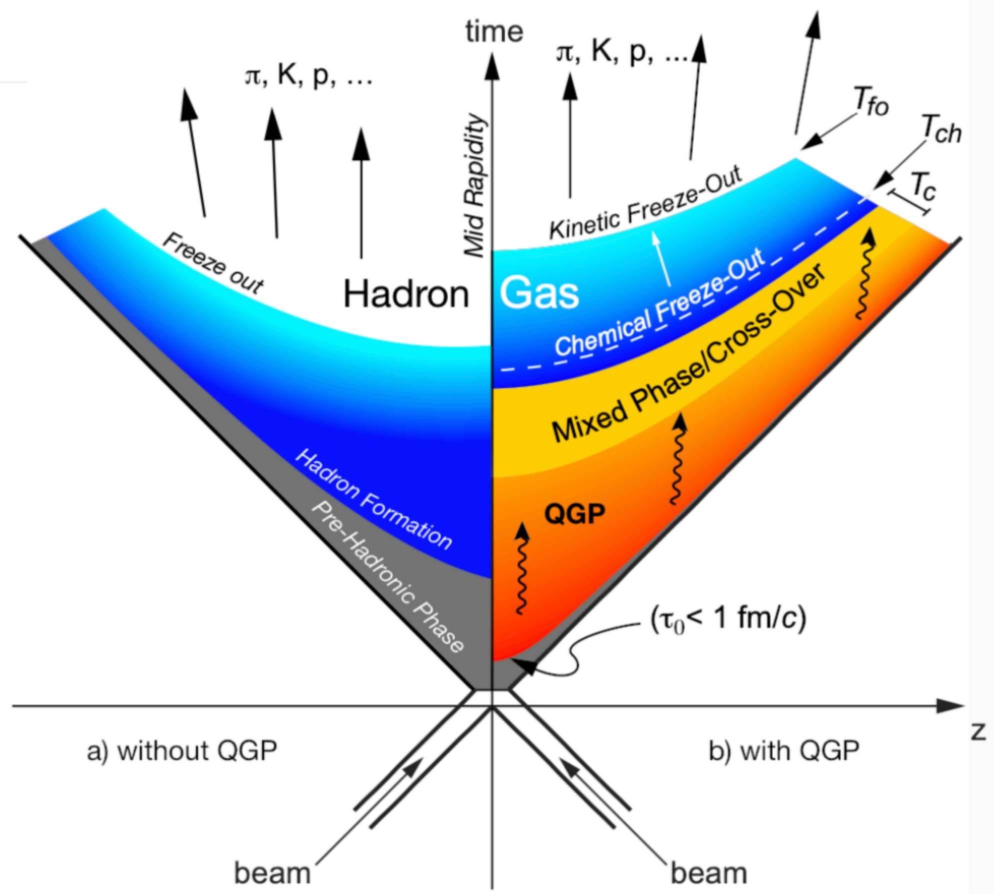

Introduction – statistical hadronization

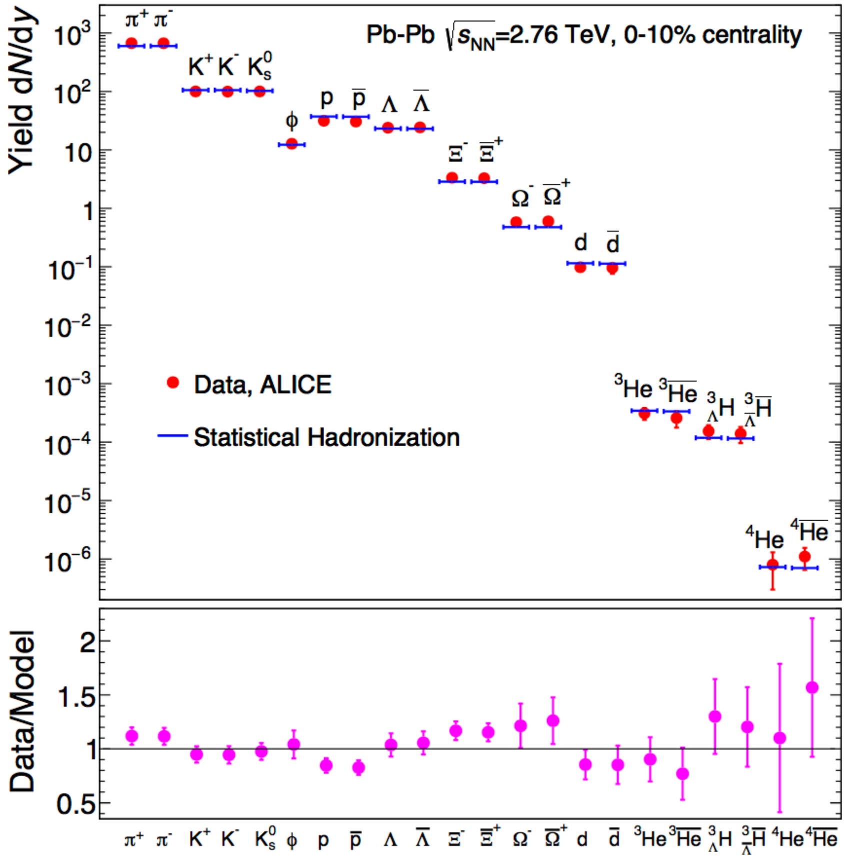

A. Andronic, P. Braun-Munzinger, K. Redlich, J.Stachel, Nature 561 (2018) 321

- Particle abundances provide information about the particle production mechanism
  →Transition from QGP to hadrons (hadronization)
- Heavier particles are produced with lower probability
  →Described well by a statistical model
- ALICE Pb-Pb data compared to Statistical Hadronization Model predictions
  →Very good agreement
- Particles and anti-particles are produced equally at the LHC ($\mu_B \approx 0$)

Introduction – production of light nuclei

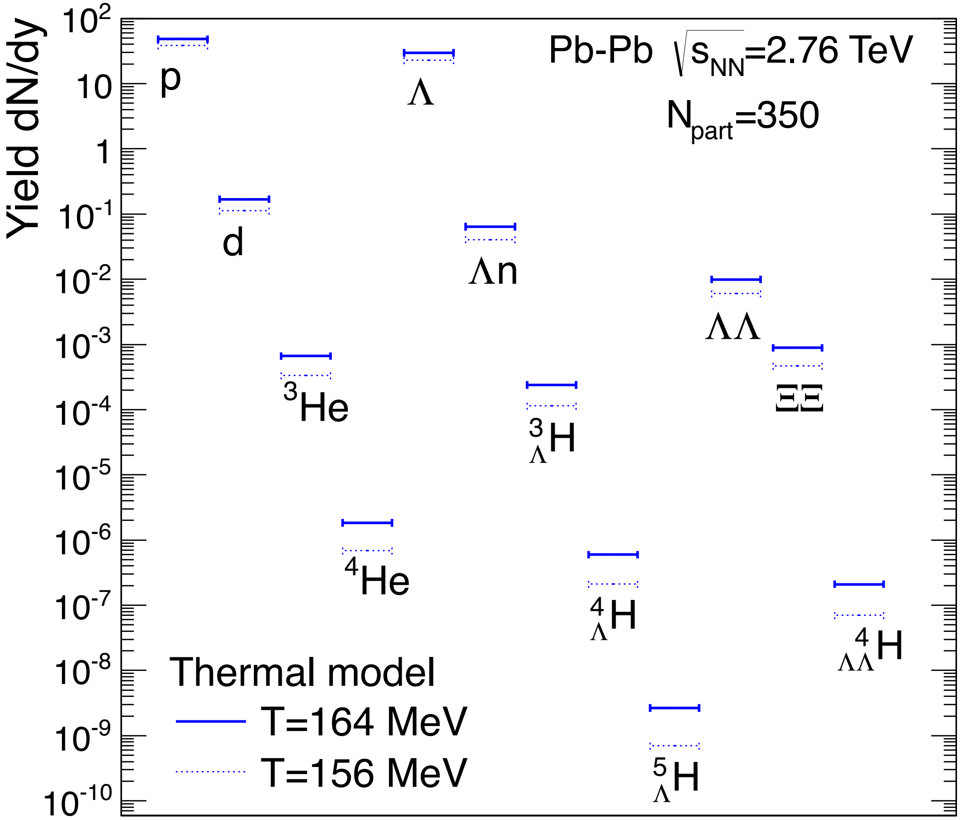

A. Andronic, private communication, model based on:
Phys. Lett. B697 (2011) 203

- Abundance of nuclei strongly sensitive to chemical freeze-out temperature T_{ch} due to
  - → Large mass
  - → Exponential dependence of the yield ~ $e^{(-m/T_{ch})}$
- Note: Binding energy of nuclei (few MeV) small compared to T_{ch}

Introduction – coalescence model

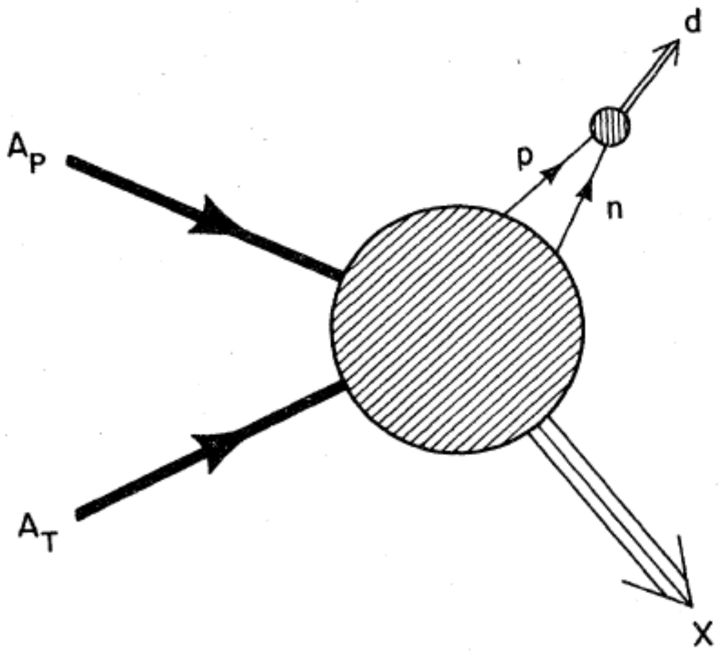

J. I. Kapusta, PRC 21, 1301 (1980)

- Nuclei are formed after kinetic freeze-out by protons and neutrons which are nearby in space and have similar velocities
  → Production rate is connected to the size of the bound state
- Nuclei can break apart and be recreated by final-state coalescence

Introduction – coalescence model

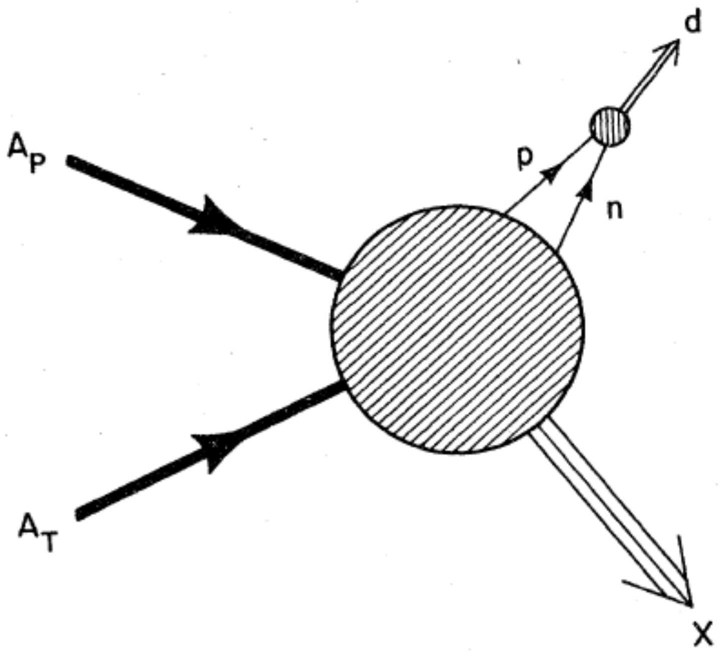

J. I. Kapusta, PRC 21, 1301 (1980)

- Main parameter of coalescence model B_A:

$$B_A = \frac{E_A \frac{\mathrm{d}^3 N_A}{\mathrm{d}^3 p_A}}{\left(E_p \frac{\mathrm{d}^3 N_p}{\mathrm{d}^3 p_p} \right)^A}$$

A: mass number of nucleus

$p_p = p_A/A$

- B_A is related to the probability to form a nucleus via coalescence

Introduction – coalescence model

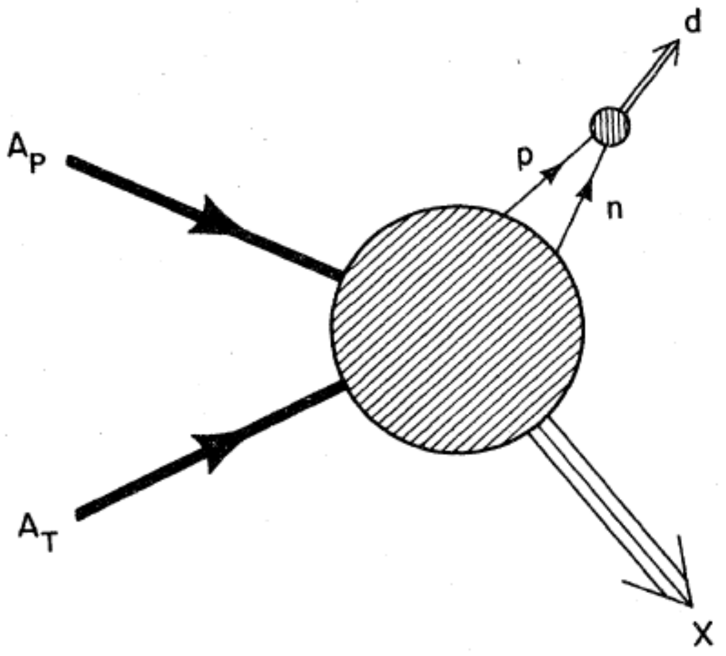

J. I. Kapusta, PRC 21, 1301 (1980)

- Main parameter of coalescence model B_A:

$$B_A = \frac{E_A \frac{d^3N_A}{d^3p_A}}{\left(E_p \frac{d^3N_p}{d^3p_p}\right)^A}$$

A: mass number of nucleus
$p_p = p_A/A$

- B_A is related to the probability to form a nucleus via coalescence

→ Nuclei are sensitive probes to constrain the production mechanism

ALICE detector setup

Inner Tracking System (ITS)
- →Vertexing
- →Tracking

Time Projection Chamber (TPC)
- →Tracking
- →Vertexing
- →Particle identification via dE/dx

Transition Radiation Detector (TRD)
- →Tracking

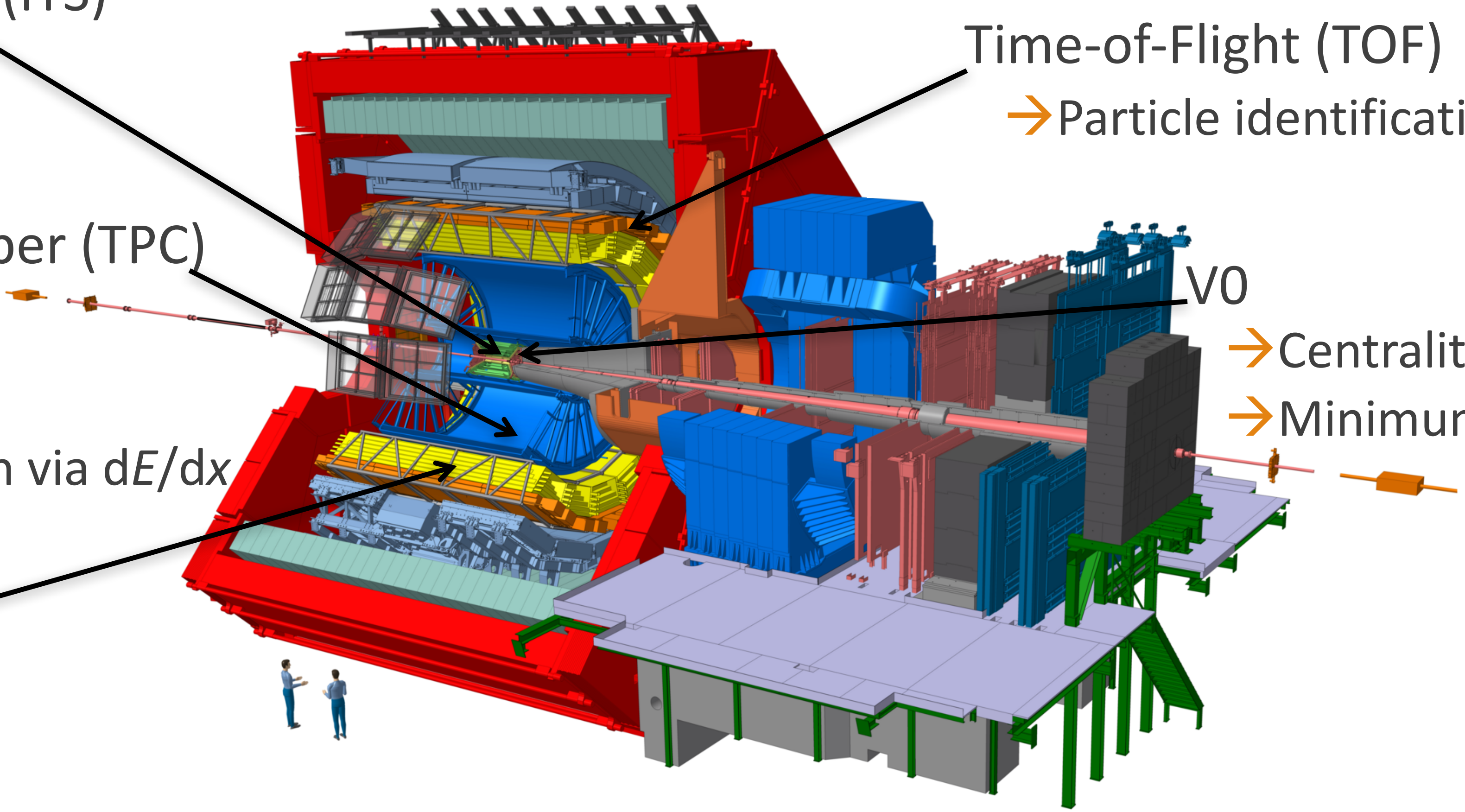

Time-of-Flight (TOF)
- →Particle identification

V0
- →Centrality determination
- →Minimum-bias trigger

Particle identification

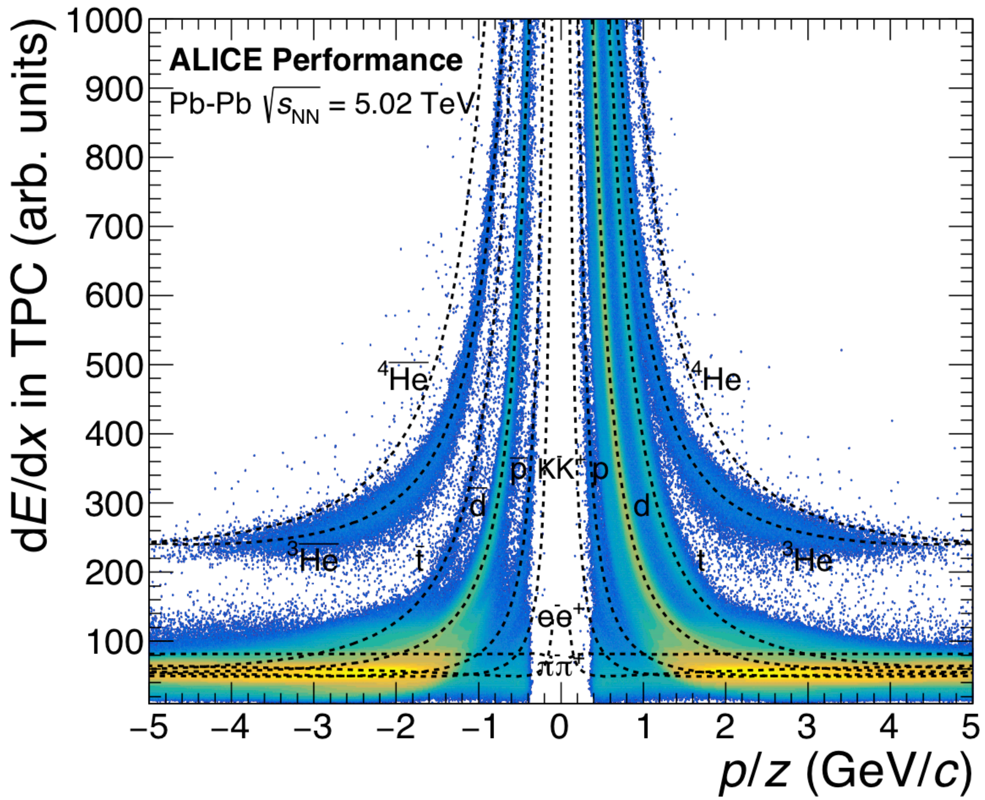

- Low momenta: TPC
  - → Nuclei identified using the energy-loss measurement

Particle identification

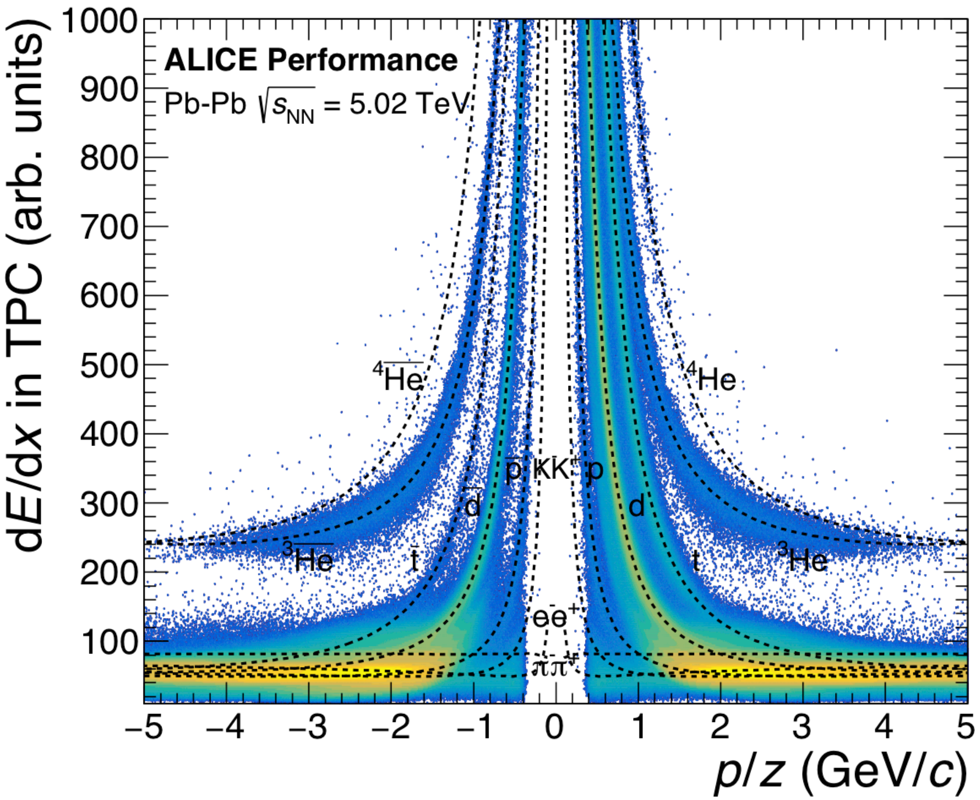

- Low momenta: TPC
  - → Nuclei identified using the energy-loss measurement
- Momentum determined from track curvature

$$\frac{p}{z} = r\,B$$

- High momenta: TOF

$$\beta = \frac{L}{t_{TOF}c}$$

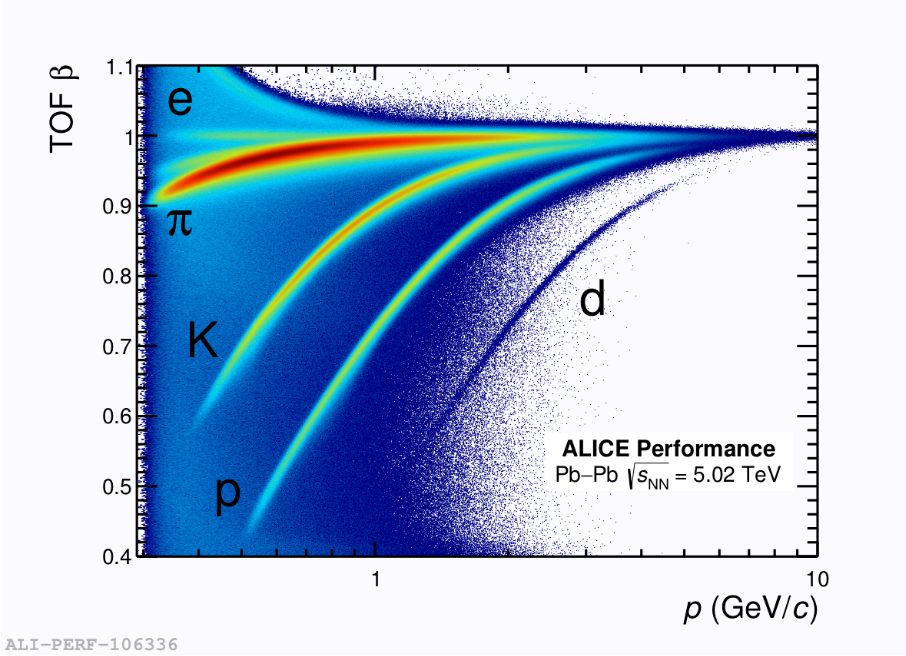

Particle identification

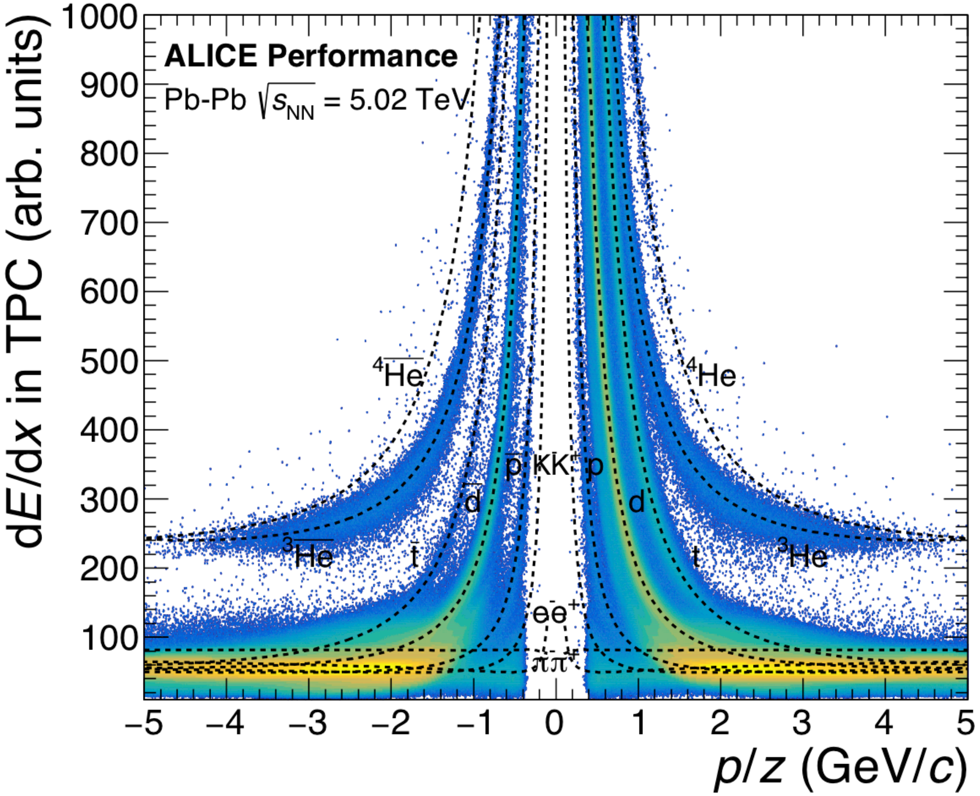

- Low momenta: TPC
  → Nuclei identified using the energy-loss measurement
- Momentum determined from track curvature

$$\frac{p}{z} = r\,B$$

- High momenta: TOF
  → m^2 distribution is calculated from the Time-of-Flight measurement

$$m^2 = \frac{(1-\beta^2)}{\beta^2}p^2$$

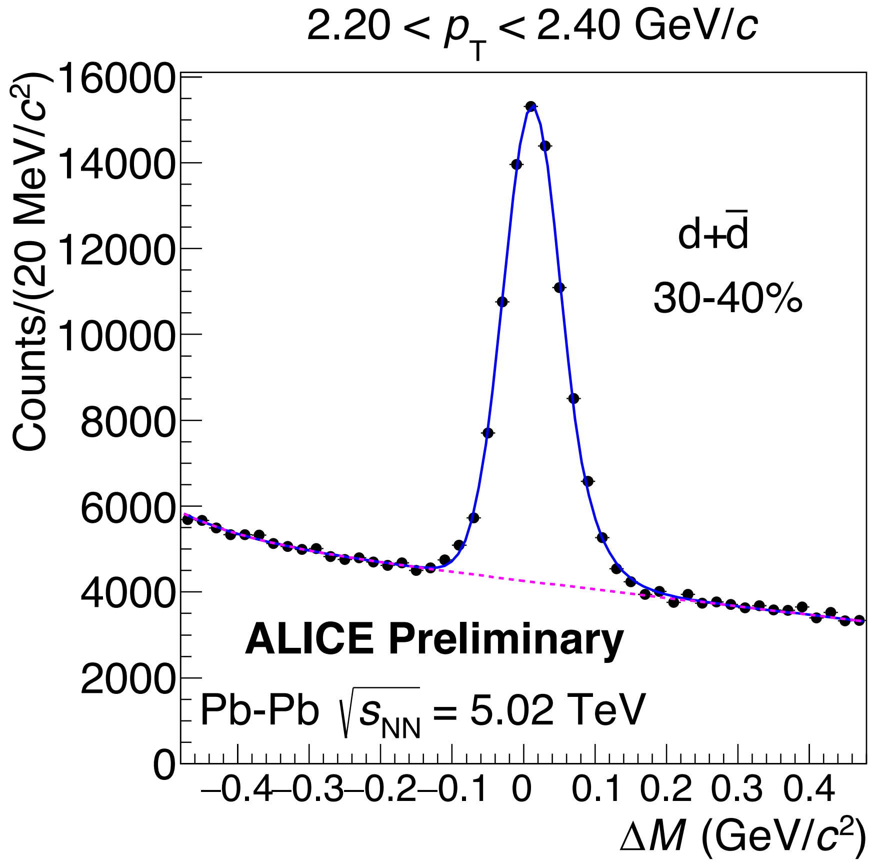

pp collisions

(Anti-)deuteron spectra

- d measured in pp collisions at $\sqrt{s_{\mathrm{NN}}}$ = 5 TeV
- d transverse momentum spectra measured in 9 multiplicity classes + minimum bias
- Expected ordering of multiplicitiy classes
- Spectra fitted with Levy-Tsallis → show no sign of radial flow

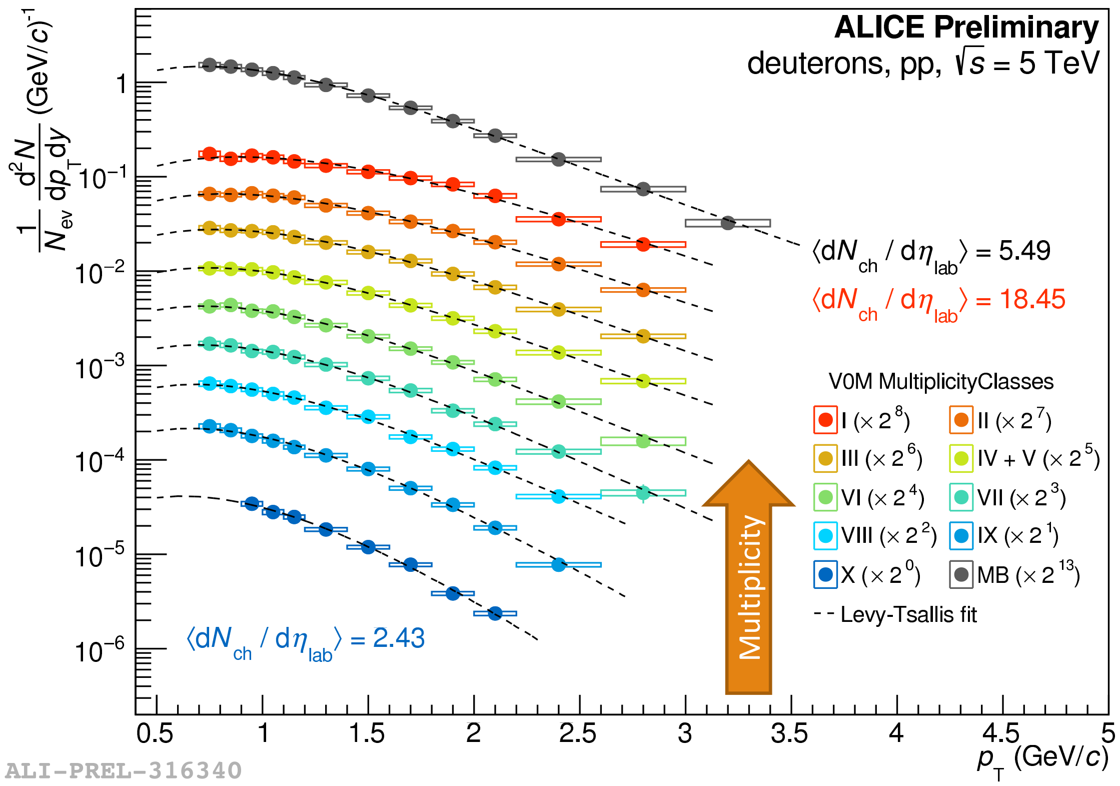

(Anti-)^{3}He spectra

- $^3\overline{\text{He}}$ and ^{3}He measured in pp collisions at $\sqrt{s_{\text{NN}}}$ = 13 TeV
- Averaged $^3\overline{\text{He}}$ and ^{3}He transverse momentum spectra measured in 2 multiplicity classes
- Expected ordering of multiplicitiy classes
- Spectra fitted with Levy-Tsallis
  → show no sign of radial flow
- $^3\overline{\text{He}}$ and ^{3}He are compatible

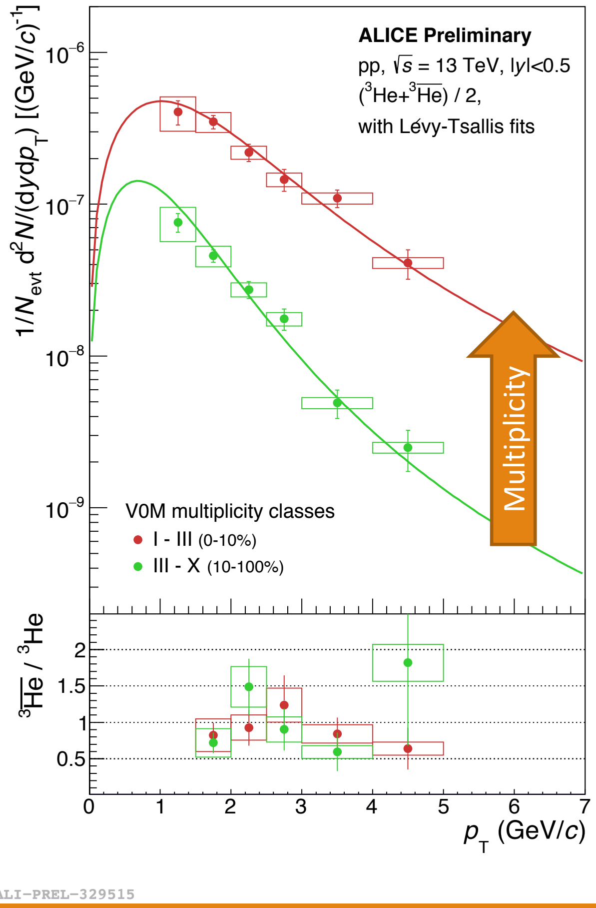

p-Pb collisions

Anti-deuteron spectra

- $\bar{d}$ measured in p-Pb collisions at $\sqrt{s_{NN}}$ = 5 TeV
- $\bar{d}$ transverse momentum spectra measured in 5 multiplicity classes
- Expected ordering of multiplicitiy classes
- Spectra well described by Blast-Wave fits
- Spectra become harder with increasing multiplicity and show clear radial flow

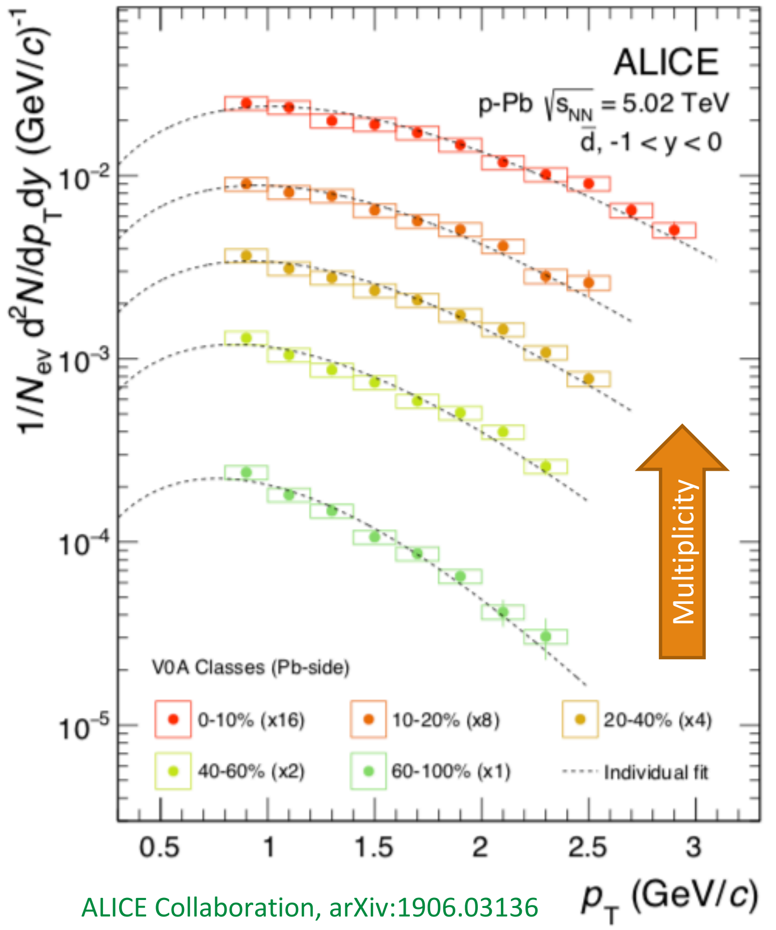

ALICE Collaboration, arXiv:1906.03136

(Anti-)^{3}He spectra

- $^3\overline{\text{He}}$ and ^{3}He measured in p-Pb collisions at $\sqrt{s_{\text{NN}}}$ = 5 TeV
- Averaged $^3\overline{\text{He}}$ and ^{3}He transverse momentum spectra measured in multiplicity classes
- Expected ordering of multiplicitiy classes

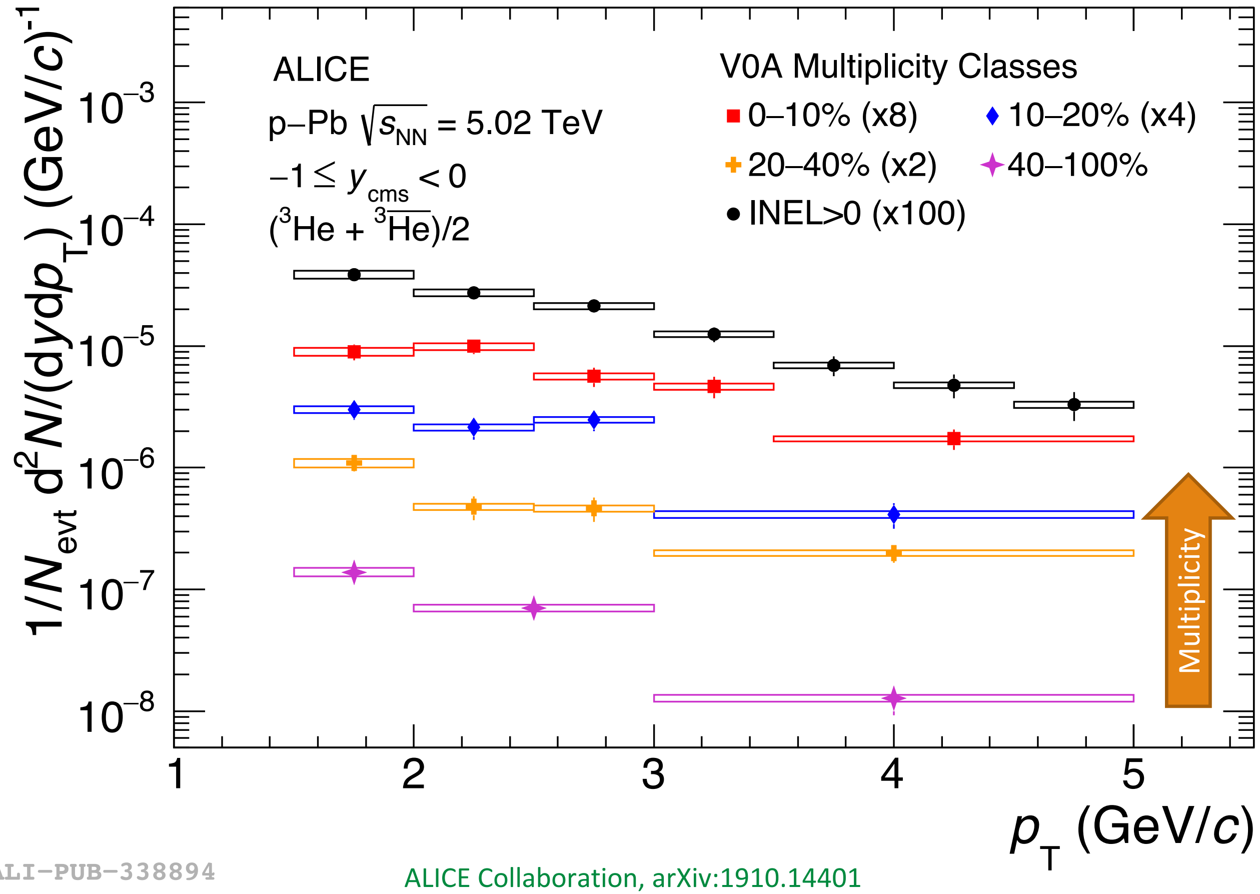

ALICE Collaboration, arXiv:1910.14401

(Anti-)t spectra compared to (anti-)^{3}He

- $\bar{t}$ and t measured in p-Pb collisions at $\sqrt{s_{NN}}$ = 5 TeV
- t and ^{3}He are compatible
  → Check of isospin symmetry in particle production
- $\bar{t}$ and t as well as $^3\overline{He}$ and ^{3}He are in agreement

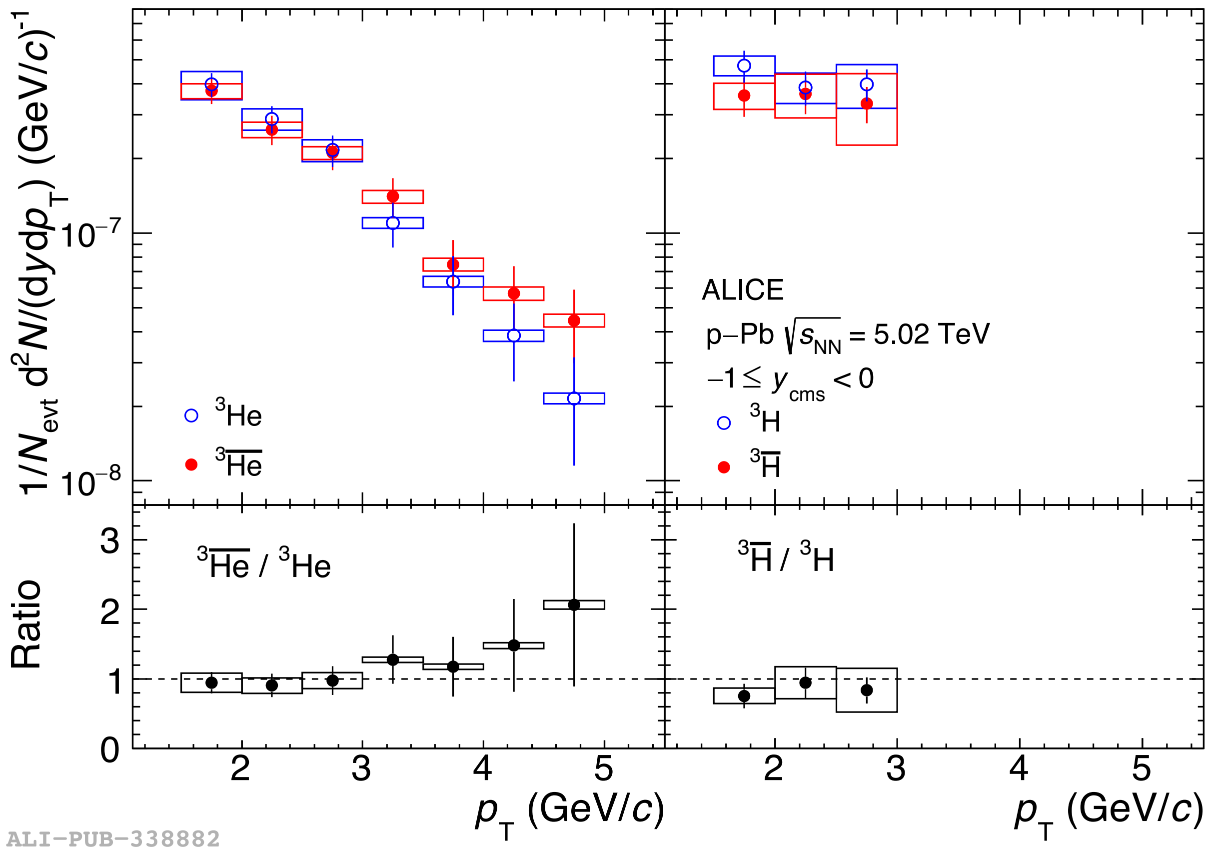

ALICE Collaboration, arXiv:1910.14401

Pb-Pb collisions

(Anti-)triton spectra

2018 high-statistics data set

- First $\bar{t}$ and t spectra in Pb-Pb at the LHC
- $\bar{t}$ and t transverse momentum spectra measured in 4 centrality intervals
- Expected ordering of centralities
- Hardening of spectra with increasing centrality
- $\bar{t}$ and t are compatible

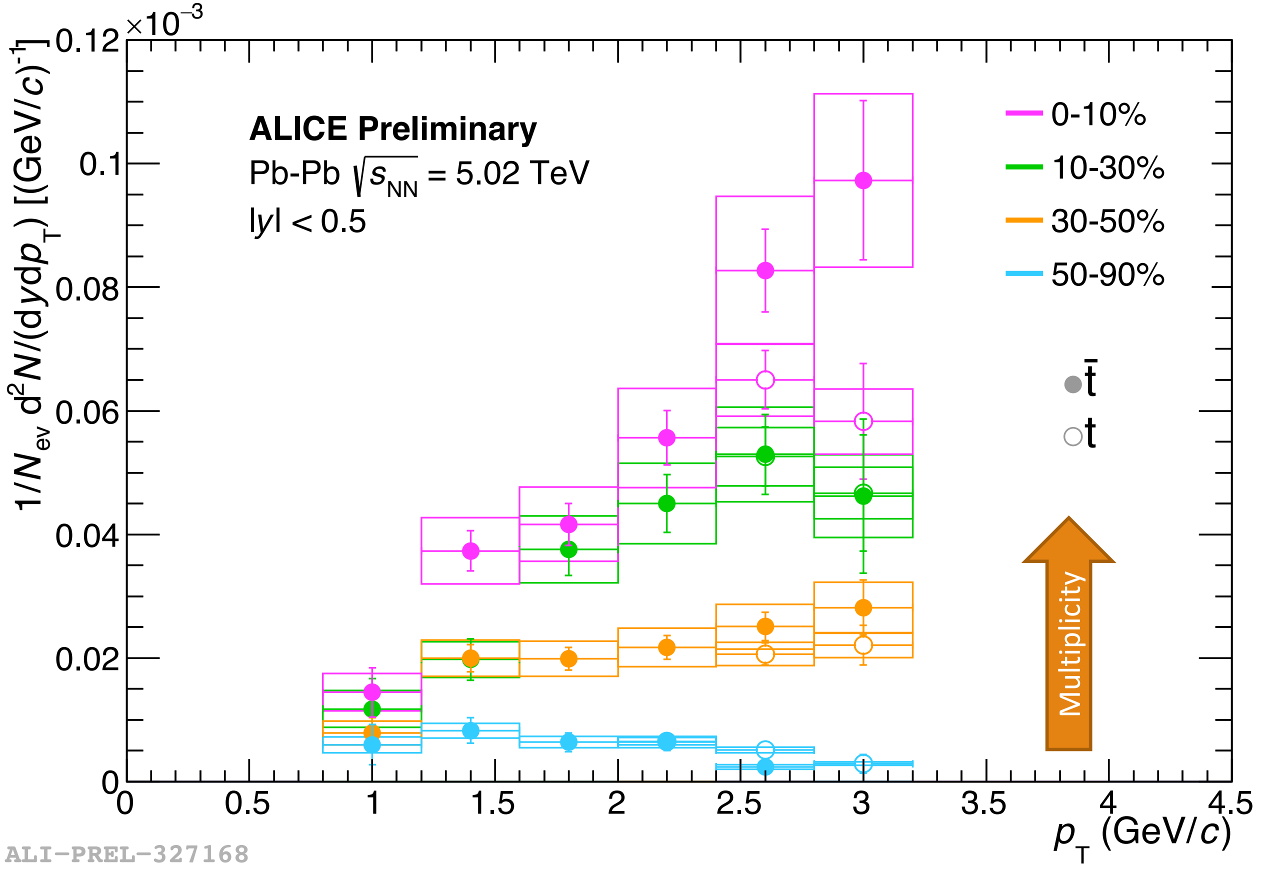

(Anti-)triton spectra

2018 high-statistics data set

- First $\bar{t}$ and t spectra in Pb-Pb at the LHC
- $\bar{t}$ and t transverse momentum spectra measured in 4 centrality intervals
- Expected ordering of centralities
- Hardening of spectra with increasing centrality
- $\bar{t}$ and t are compatible
- Integrated production yield (d*N*/dy) extracted from Blast-Wave fits

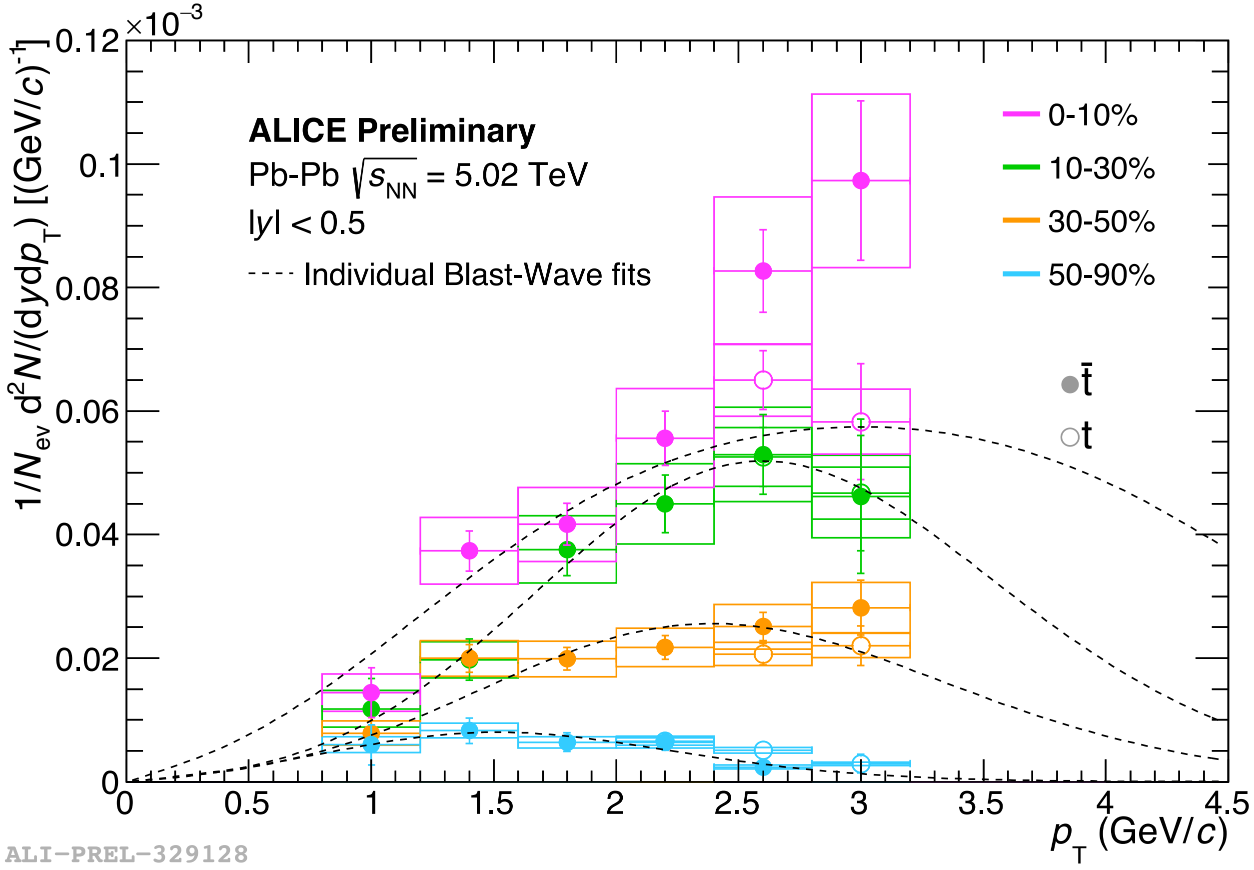

(Anti-)^{3}He spectra

- $^3\overline{\text{He}}$ and ^{3}He measured in Pb-Pb collisions at $\sqrt{s_{\text{NN}}}$ = 5 TeV
- $^3\overline{\text{He}}$ and ^{3}He transverse momentum spectra measured in 3 centrality intervals
- Expected ordering of centralities
- Hardening of spectra with increasing centrality
- Integrated production yield (dN/dy) extracted from Blast-Wave fits

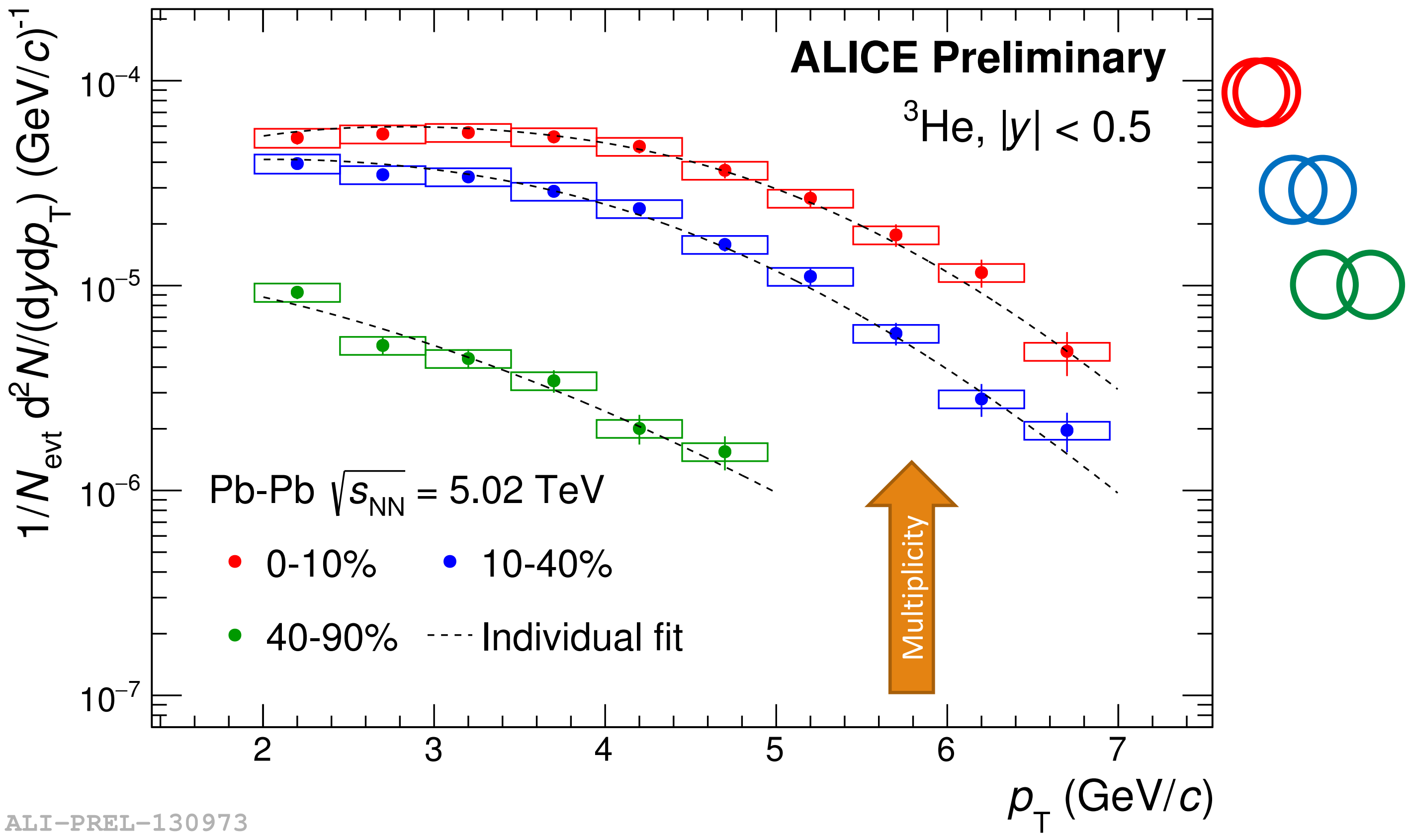

Deuteron spectra

- d measured in Pb-Pb collisions at $\sqrt{s_{NN}}$ = 5 TeV
- d transverse momentum spectra measured in 10 centrality intervals
- Expected ordering of centralities
- Hardening of spectra with increasing centrality
- Integrated production yield (dN/dy) extracted from Blast-Wave fits

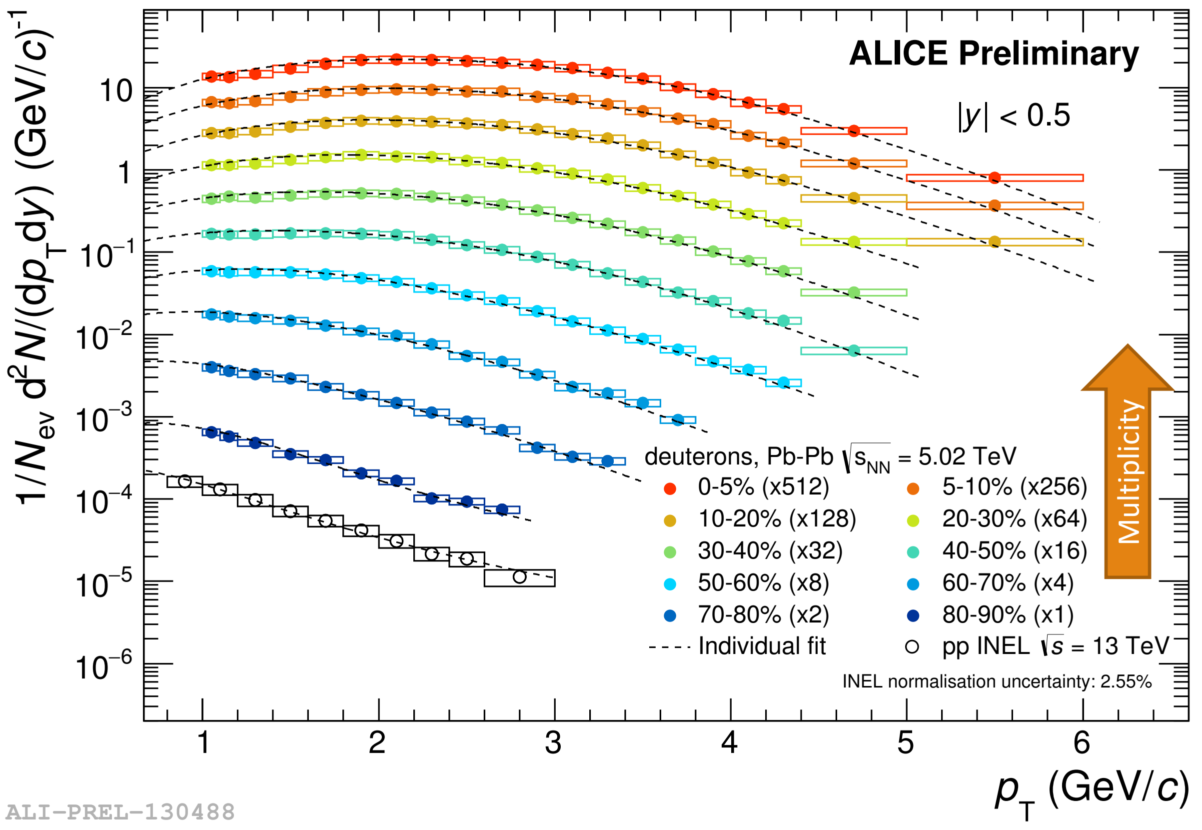

(Anti-)^{4}He signal extraction

2018 high-statistics data set

- $^4\overline{\text{He}}$ and ^{4}He measured in the 0-10 % most central collisions
- ^{3}He and ^{4}He clearly separated in TOF mass (m^2/z^2 (^{4}He)= 3.475 GeV$^2/c^4$)
- Background from mismatches (magenta) and contribution from ^{3}He (dashed line) subtracted from the ^{4}He yield

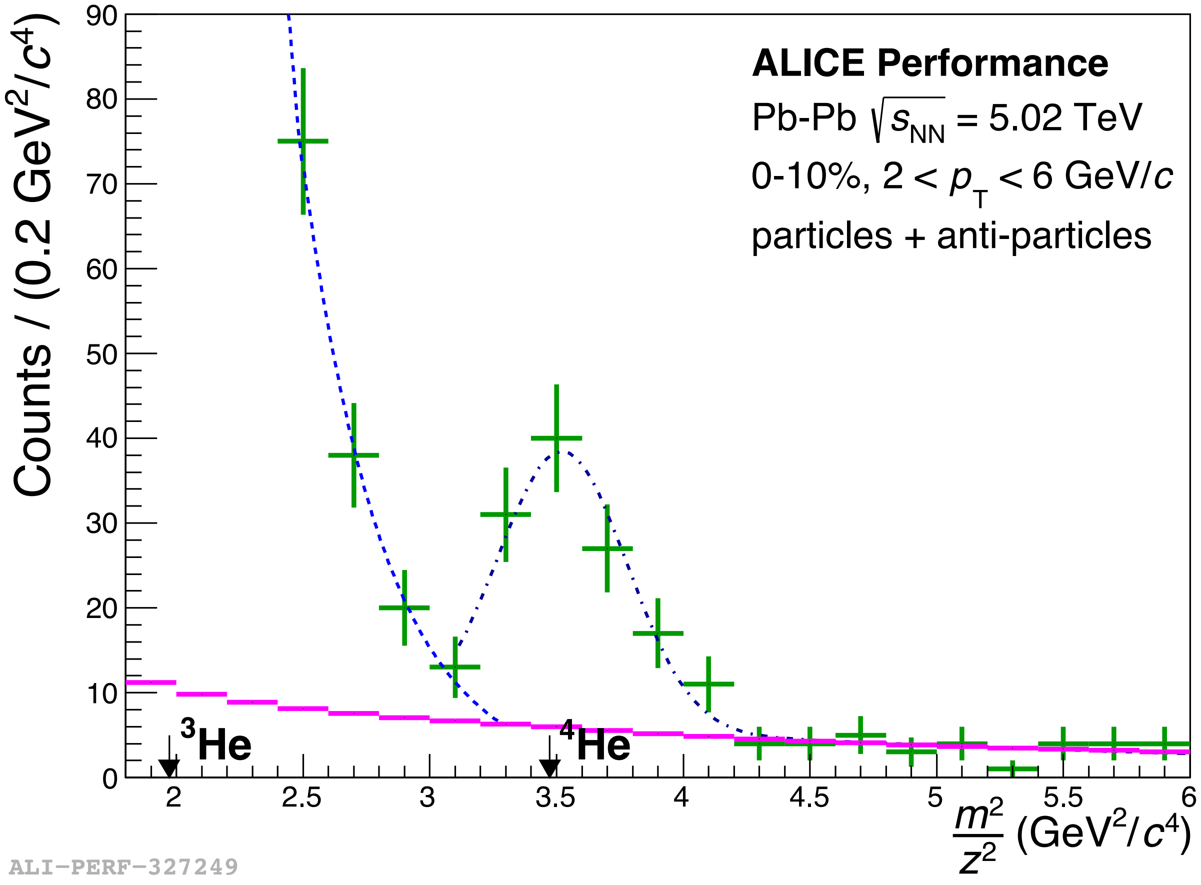

(Anti-)^{4}He

2018 high-statistics data set

- First $^4\overline{\text{He}}$ and ^{4}He transverse momentum spectra measured at the LHC
- Yield extracted in the 0-10 % most central collisions in 4 p_T bins from 2 to 6 GeV/c

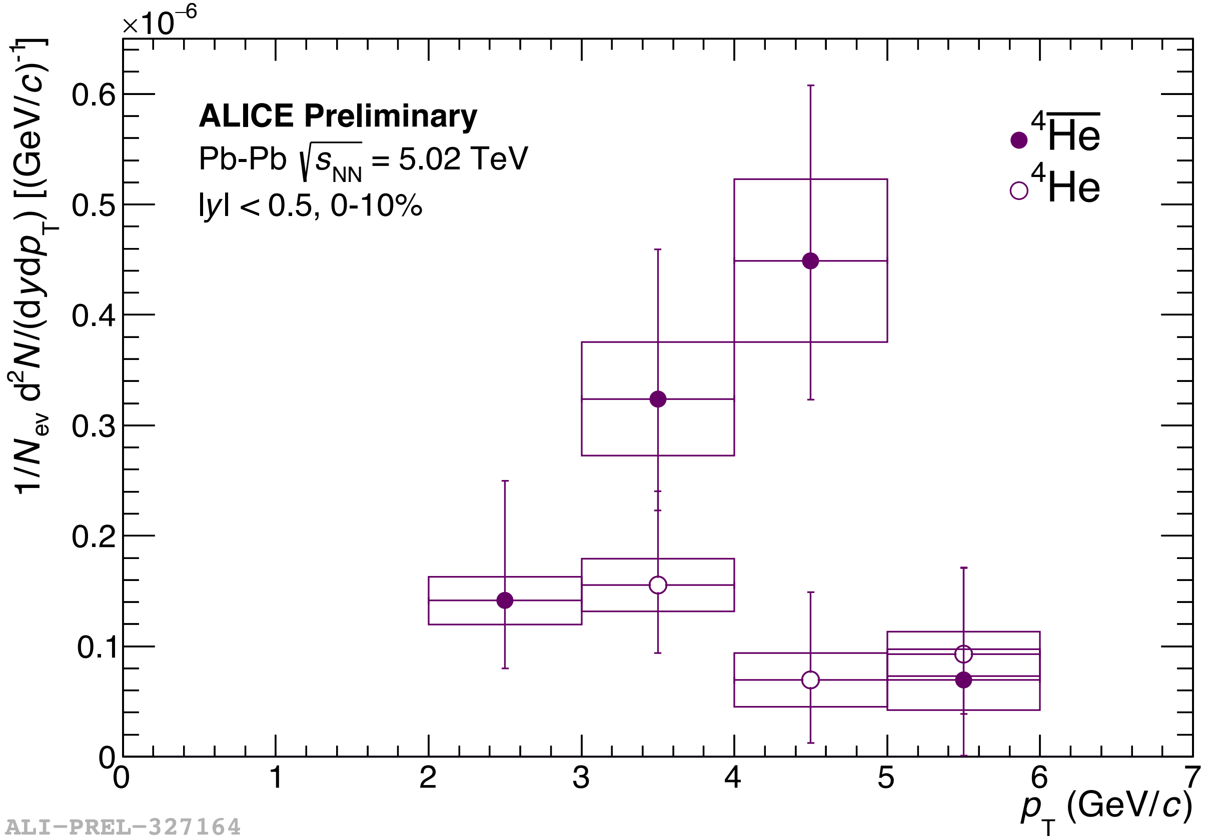

Thermal model fits

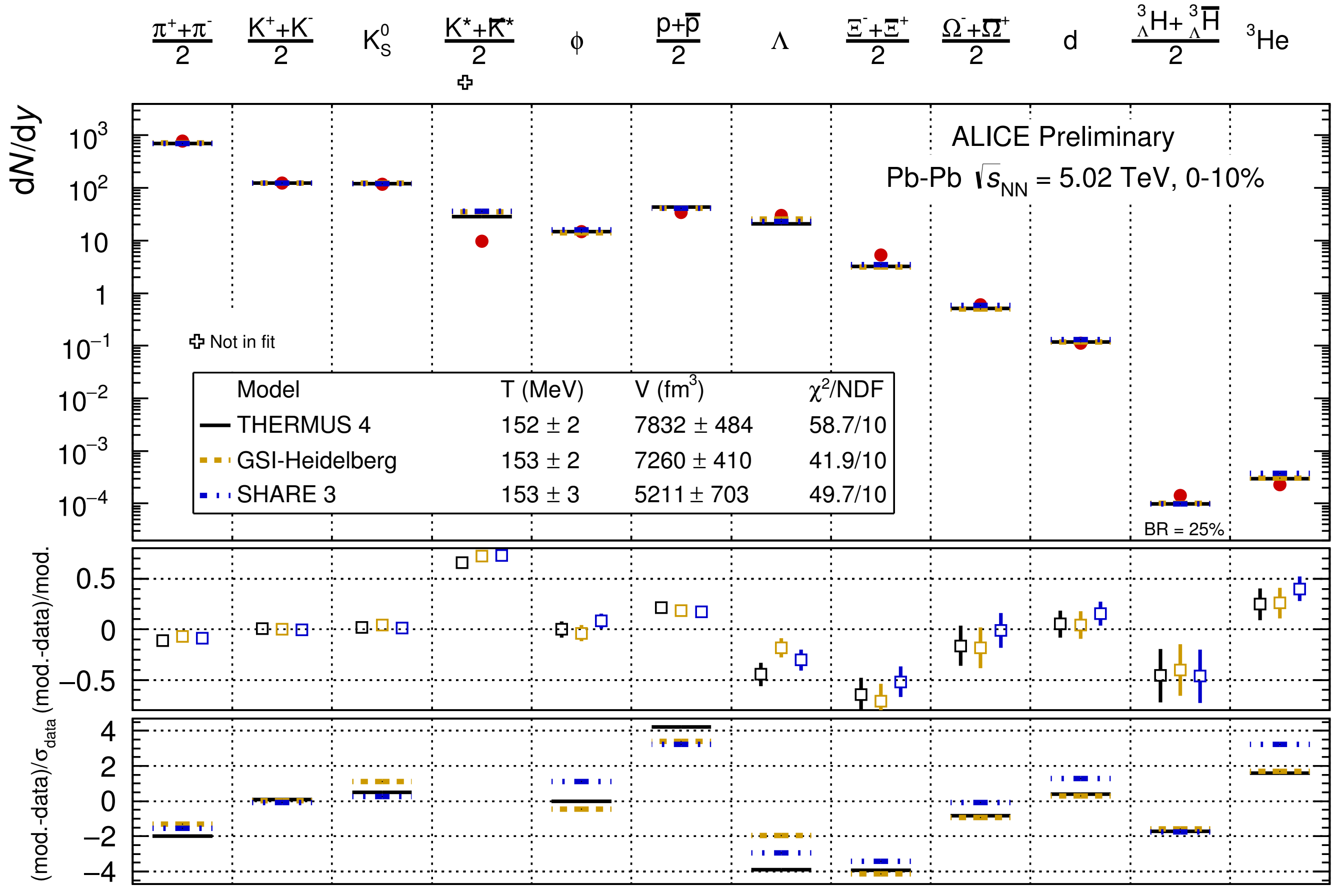

ALI-PREL-148739 ALICE Collaboration, arXiv:1910.07678

- Different model variants describe particle yields including light (hyper-)nuclei well with T_{ch} of about 153 MeV

Thermal model fits

2018 high-statistics data set

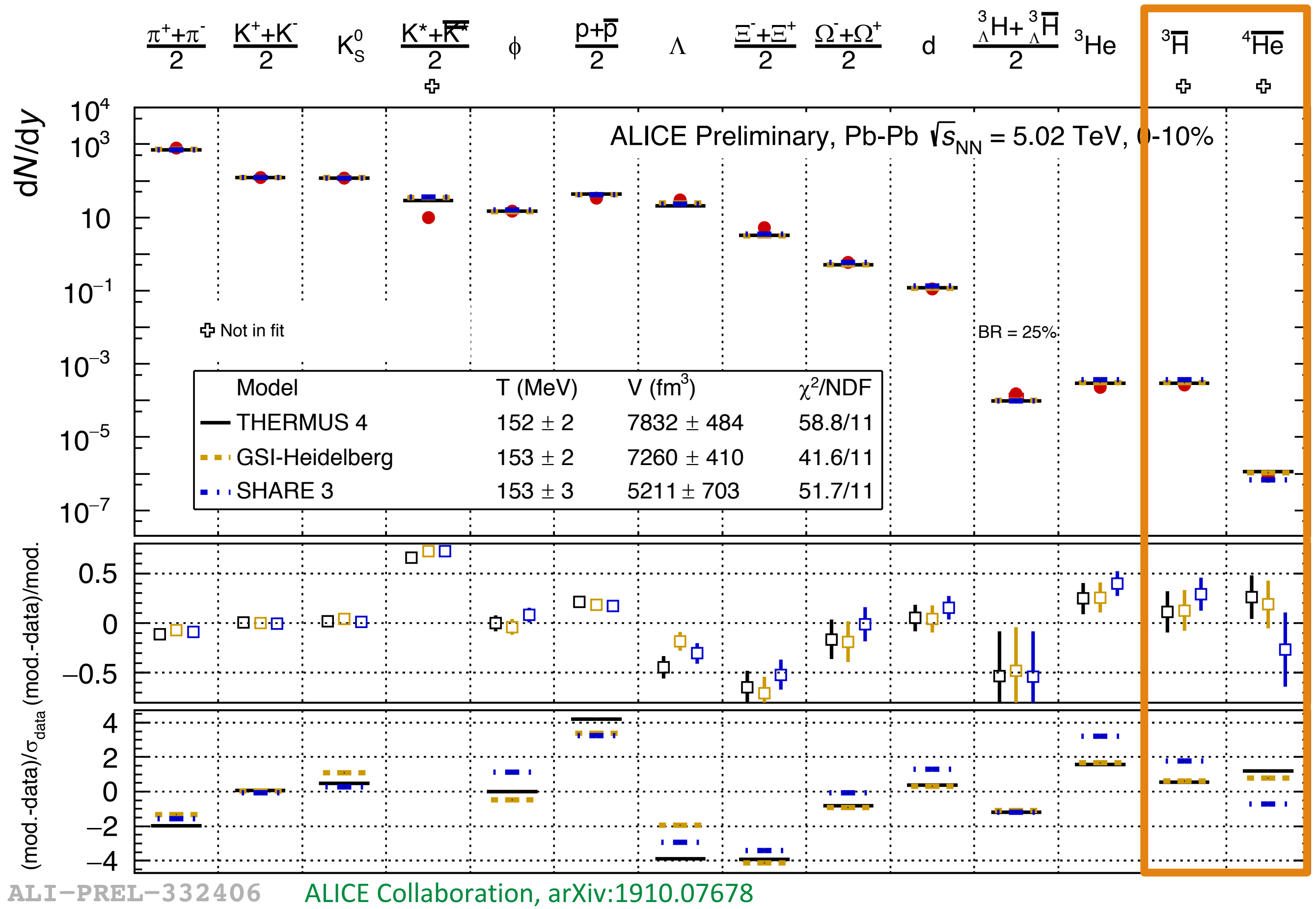

ALICE Collaboration, arXiv:1910.07678

- Different model variants describe particle yields including light (hyper-)nuclei well with T_{ch} of about 153 MeV
- $\bar{t}$ and $^{4}\overline{He}$ not included in the fit
  → In good agreement with the prediction from fit to other light-flavoured particles

Combined Blast-Wave fits

2018 high-statistics data set

- Simultaneous Blast-Wave fit of $\pi^{\pm}$, $K^{\pm}$, p, d, $\bar{t}$, ^{3}He and $^{4}\overline{\text{He}}$ spectra in central Pb-Pb collisions describes all particles quite well
- Spectra show clear radial flow
  → common flow velocity ⟨β⟩ and kinetic freeze-out temperature T_{kin}

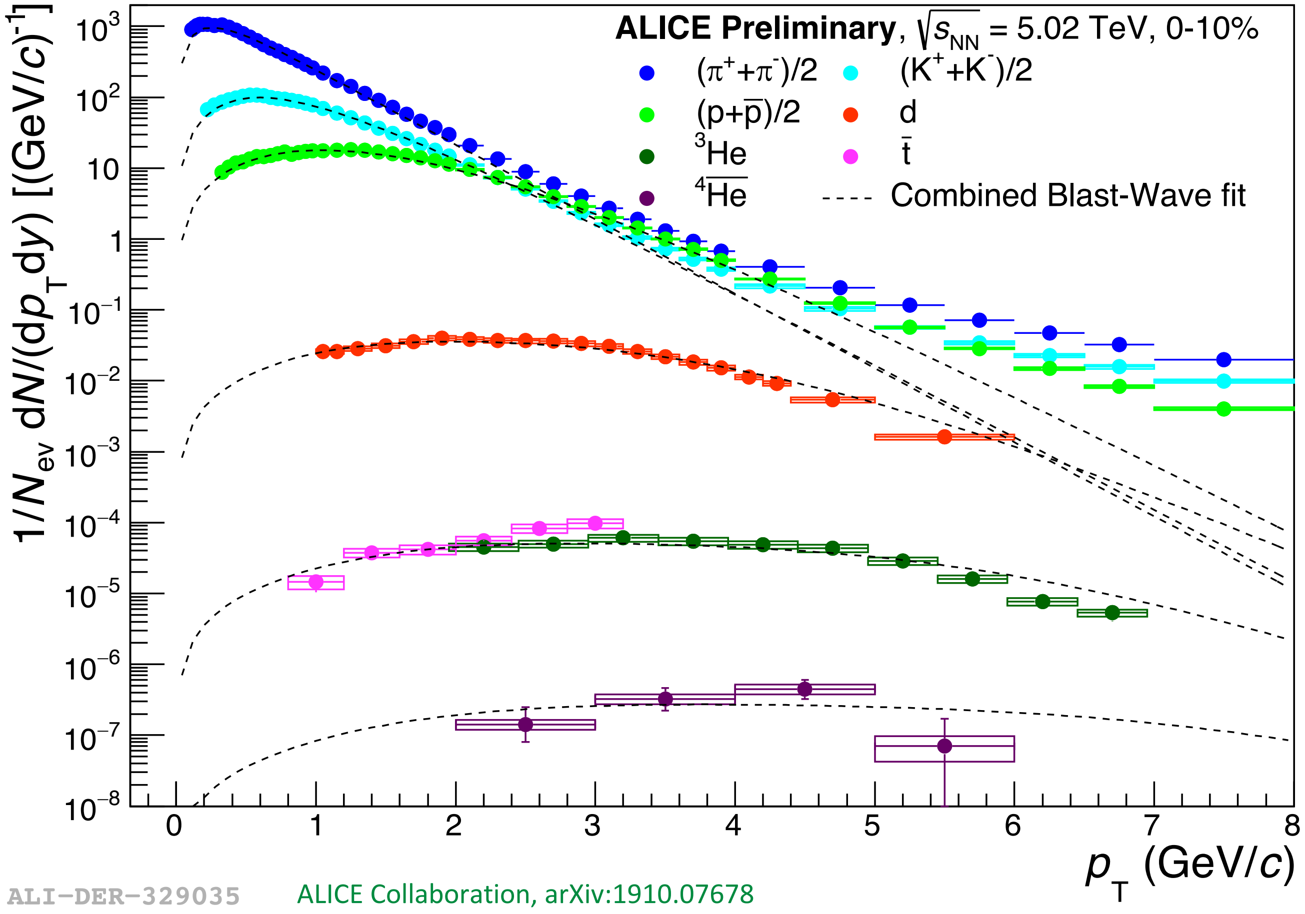

ALICE Collaboration, arXiv:1910.07678

Elliptic flow

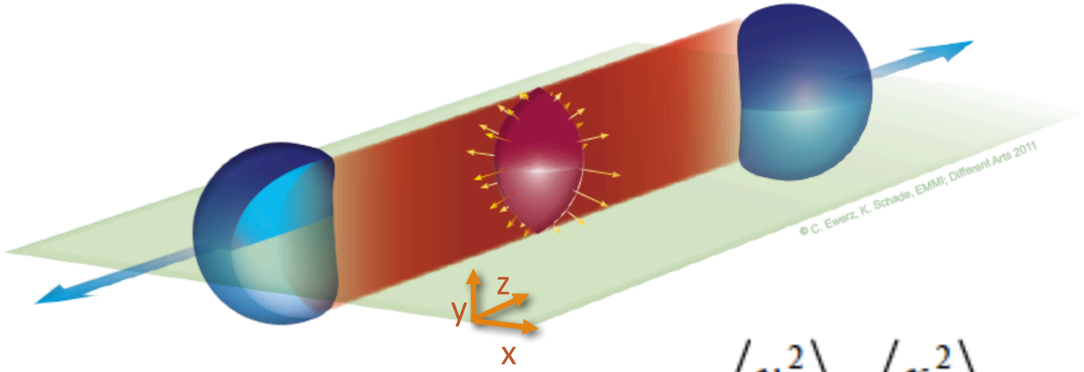

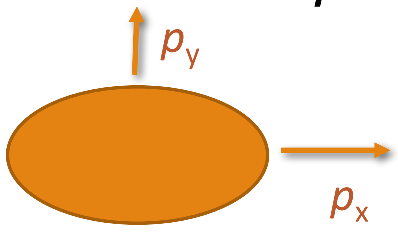

$$\boldsymbol{\phi} = \arctan\frac{p_y}{p_x}$$

$$\varepsilon = \frac{\langle y^2\rangle - \langle x^2\rangle}{\langle y^2\rangle + \langle x^2\rangle} \Rightarrow v_2 = \left\langle \frac{p_x^{\,2} - p_y^{\,2}}{p_x^{\,2} + p_y^{\,2}} \right\rangle$$

Coordinate-space anisotropy | Momentum-space anisotropy

$$\frac{dN}{d\phi} \propto 1 + 2v_2\cos[2(\phi - \Psi_R)] + 2v_4\cos[4(\phi - \Psi_R)] + \ldots$$

Elliptic flow term

Fourier transformation

(Anti-)^{3}He elliptic flow

- $^3\overline{He}$ and ^{3}He elliptic flow versus transverse momentum extracted in 3 centrality intervals
- Elliptic flow is increasing going from central to more peripheral collisions, because of the increasing asymmetry of the overlap region of the colliding nuclei
- Elliptic flow is increasing with p_T

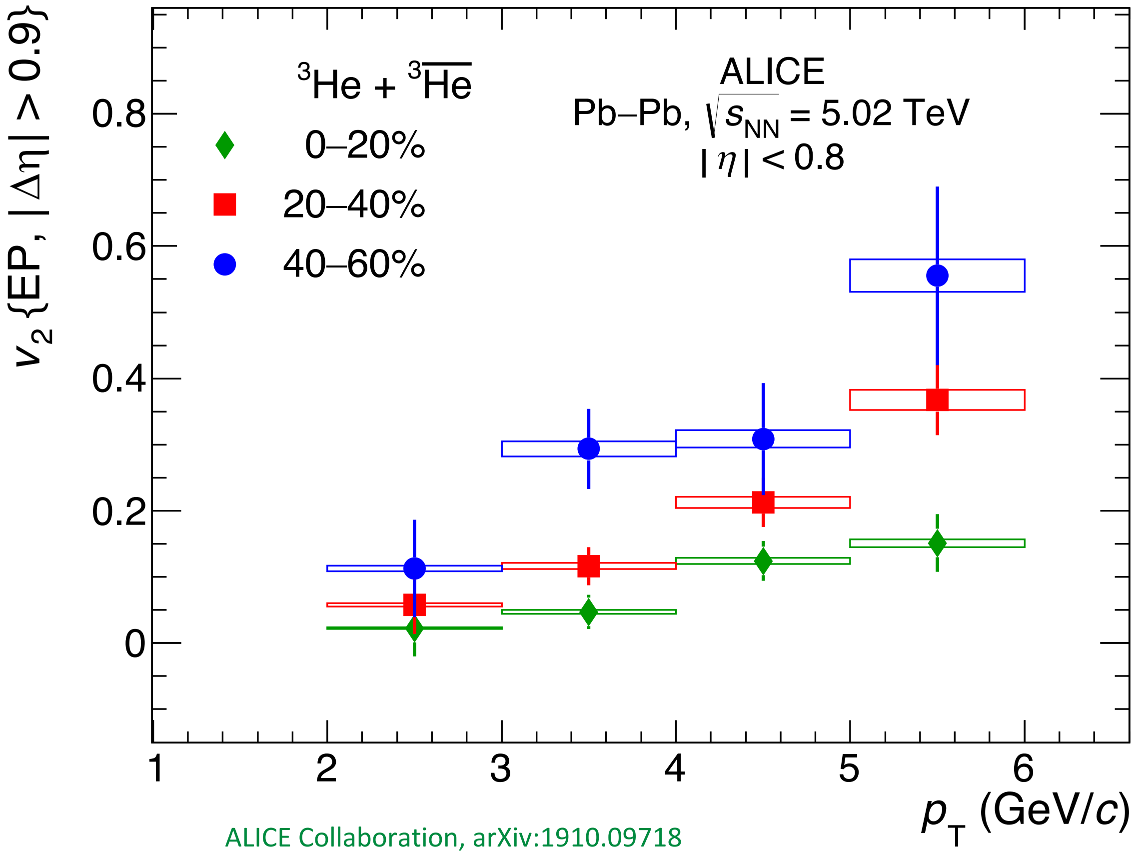

ALICE Collaboration, arXiv:1910.09718

Comparison of elliptic flow

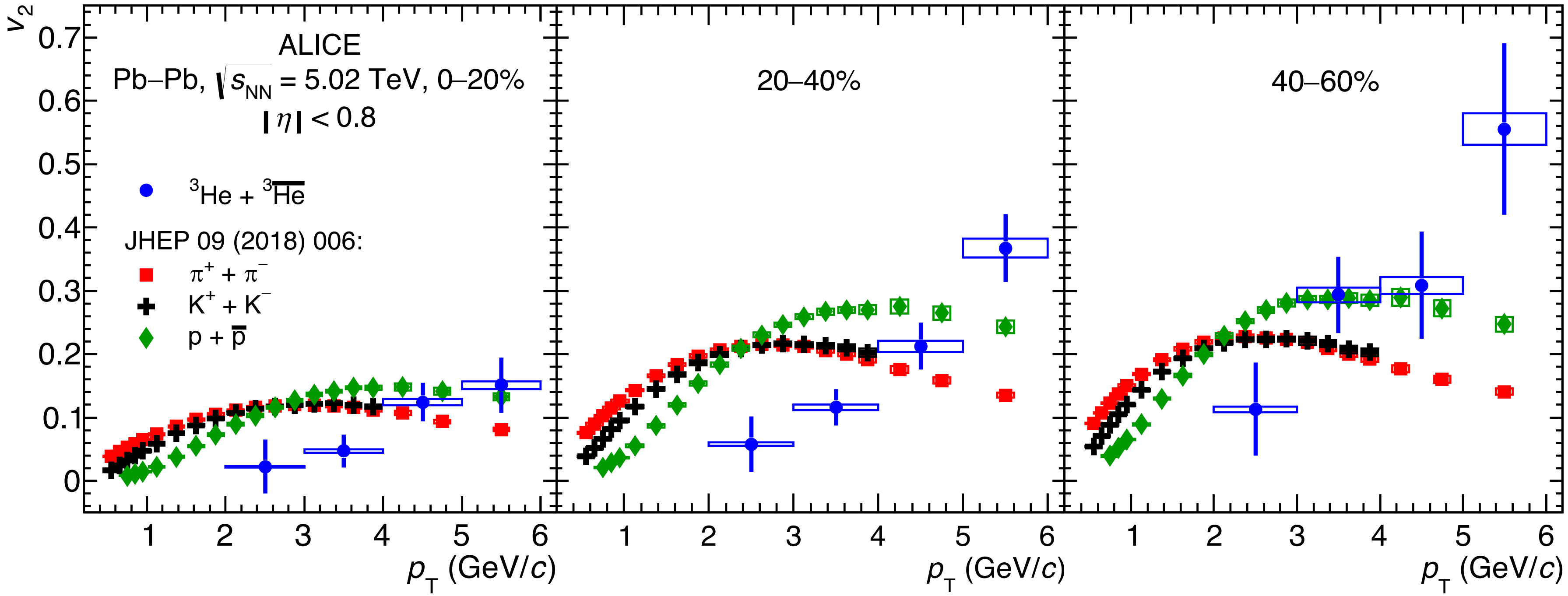

ALICE Collaboration, arXiv:1910.09718

- v_2 of ^{3}He compared to π, K and p at the same center-of-mass energy
- Clear mass ordering observed as expected from hydrodynamics

Comparison with Blast-Wave and coalescence model

- Blast-Wave fit of π, K and p used to predict ^3He elliptic flow
- Naïve coalescence model using simple scaling of v_2 and p_T
- Data between the two models in all three centrality intervals

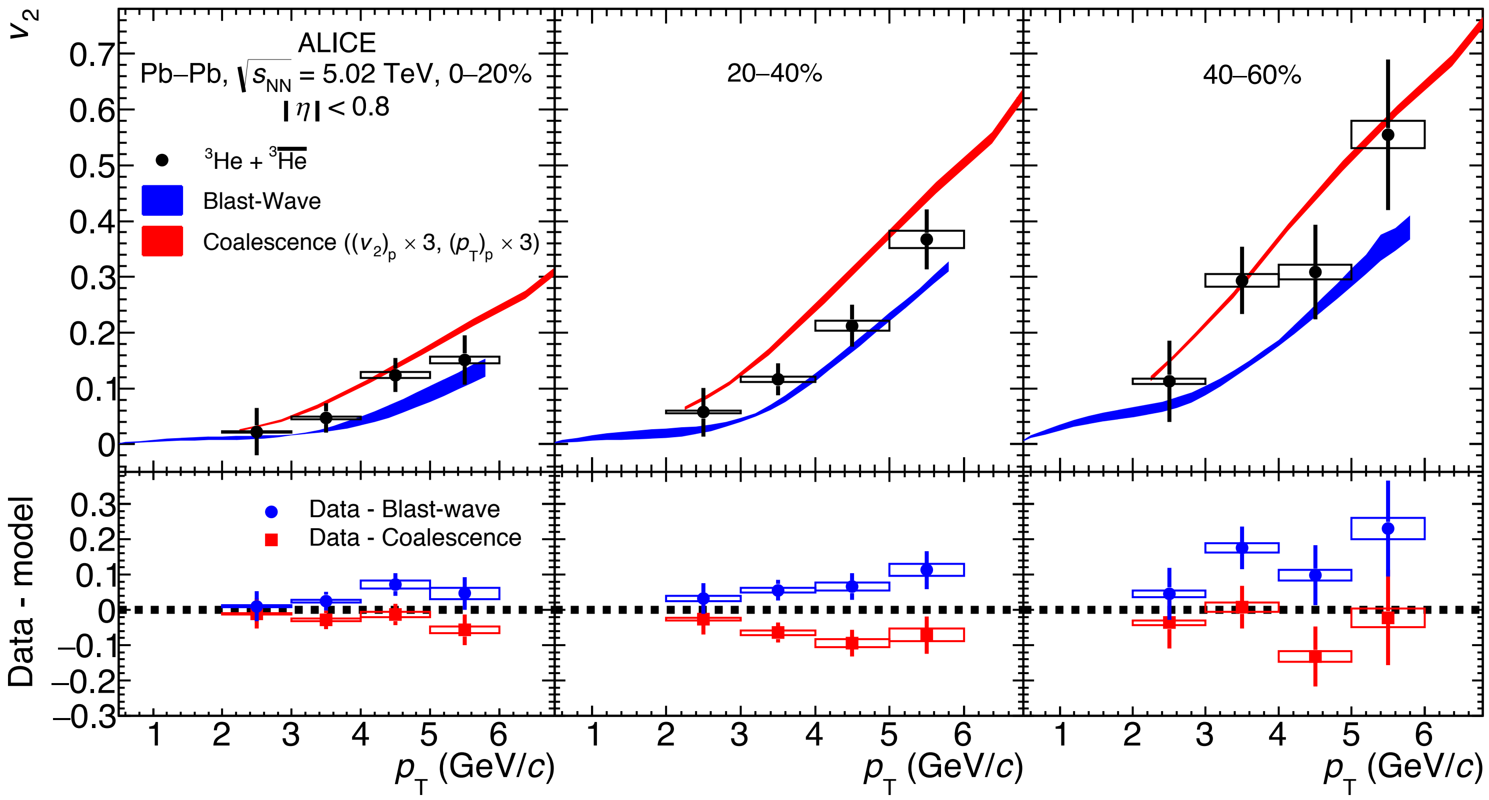

ALICE Collaboration, arXiv:1910.09718

Comparison to more sophisticated coalescence model

- Data in 0-20 % and 20-40 % centrality intervals compared to iEBE-VISHNU hybrid model with AMPT initial conditions
  - → Phase-space distribution of p and n taken into account
  - → Hybrid model of viscous hydrodynamics where nuclei are formed by final-state coalescence
- Data and model are in good agreement

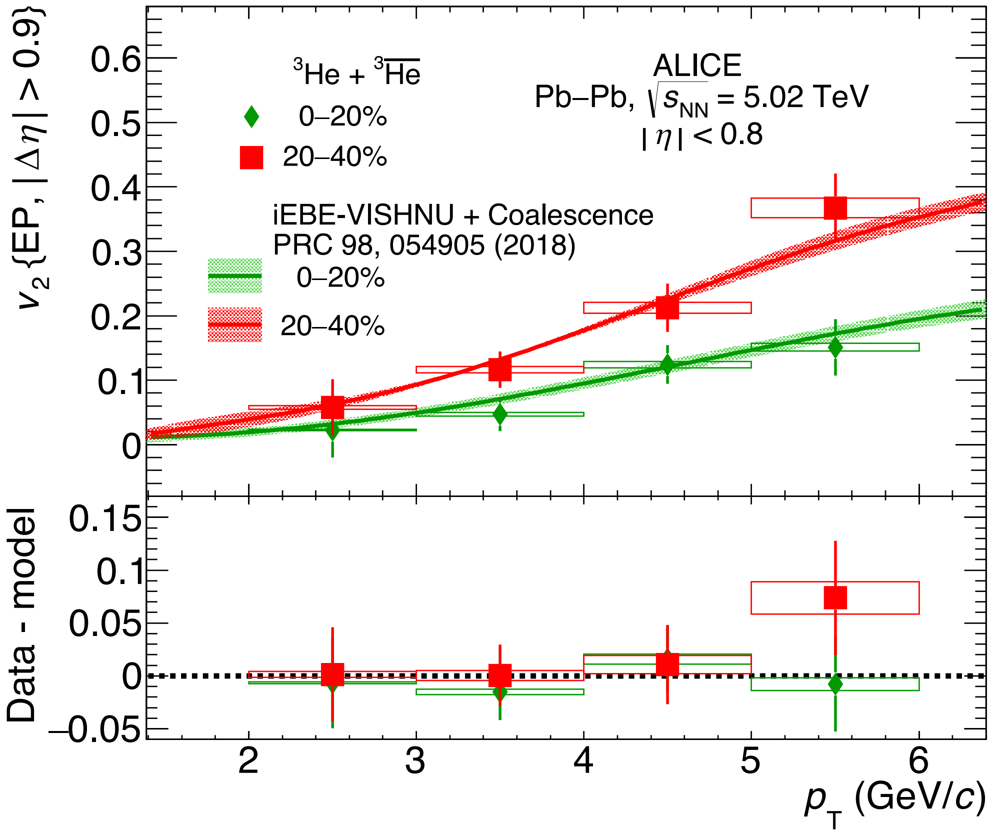

ALICE Collaboration, arXiv:1910.09718

Coalescence parameters

The coalescence parameter B_2

- The probability to form a nucleus can be quantified by the coalescence parameter B_A

$$B_A = \frac{E_A \frac{d^3N_A}{d^3p_A}}{\left(E_p \frac{d^3N_p}{d^3p_p}\right)^A}$$

- According to simple coalescence predictions B_A is flat in p_T
  → This is the case for pp collisions

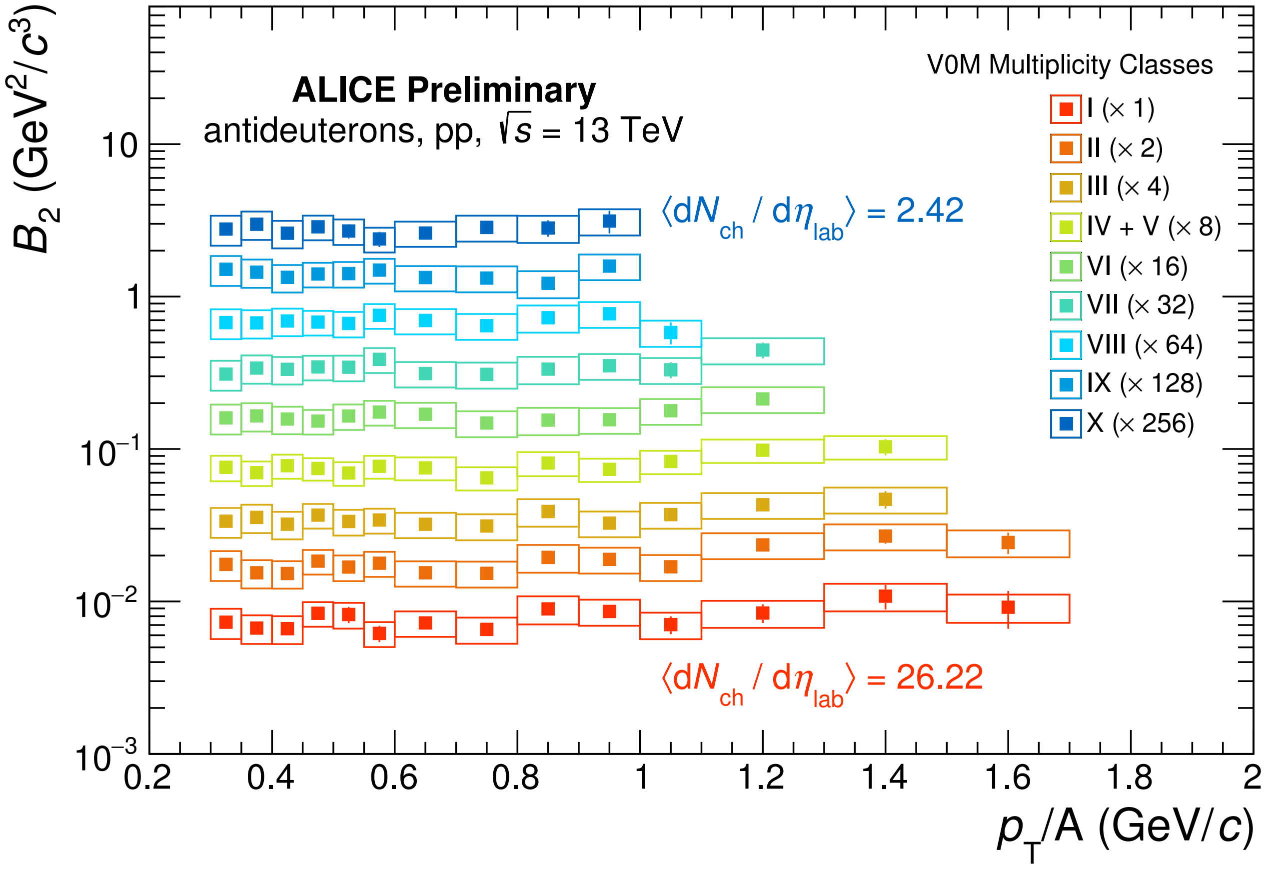

ALI-PREL-146141

The coalescence parameter B_2

- However, this is not the case in Pb-Pb collisions
  → Rise in p_T

- Moving from central to more peripheral collisions (i.e. towards lower multiplicities) the rise in p_T becomes milder

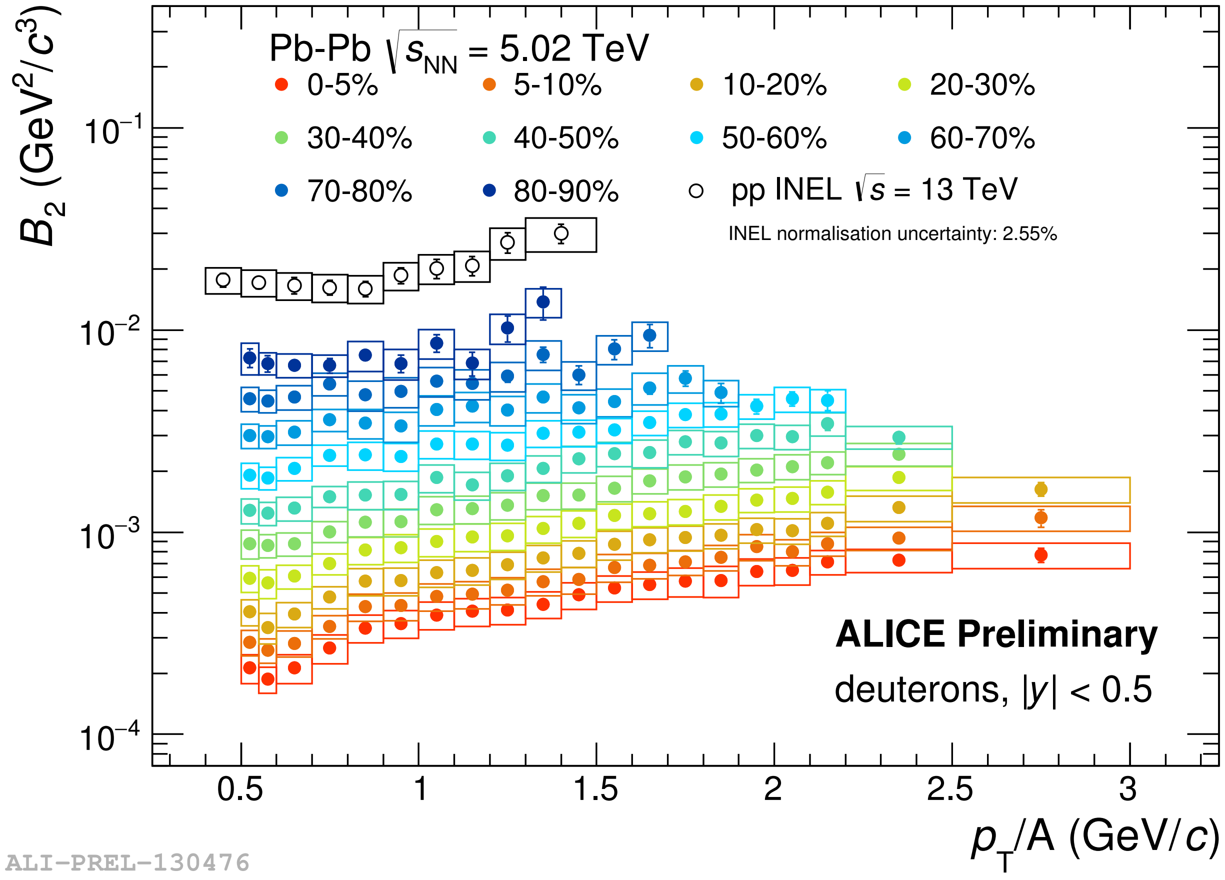

The coalescence parameter B_3

- In p-Pb collisions rise in p_T observed

- B_3 has also been measured in different collision systems

- Comparison of B_3 in different collision systems
  → Dependence of coalescent production of the system size

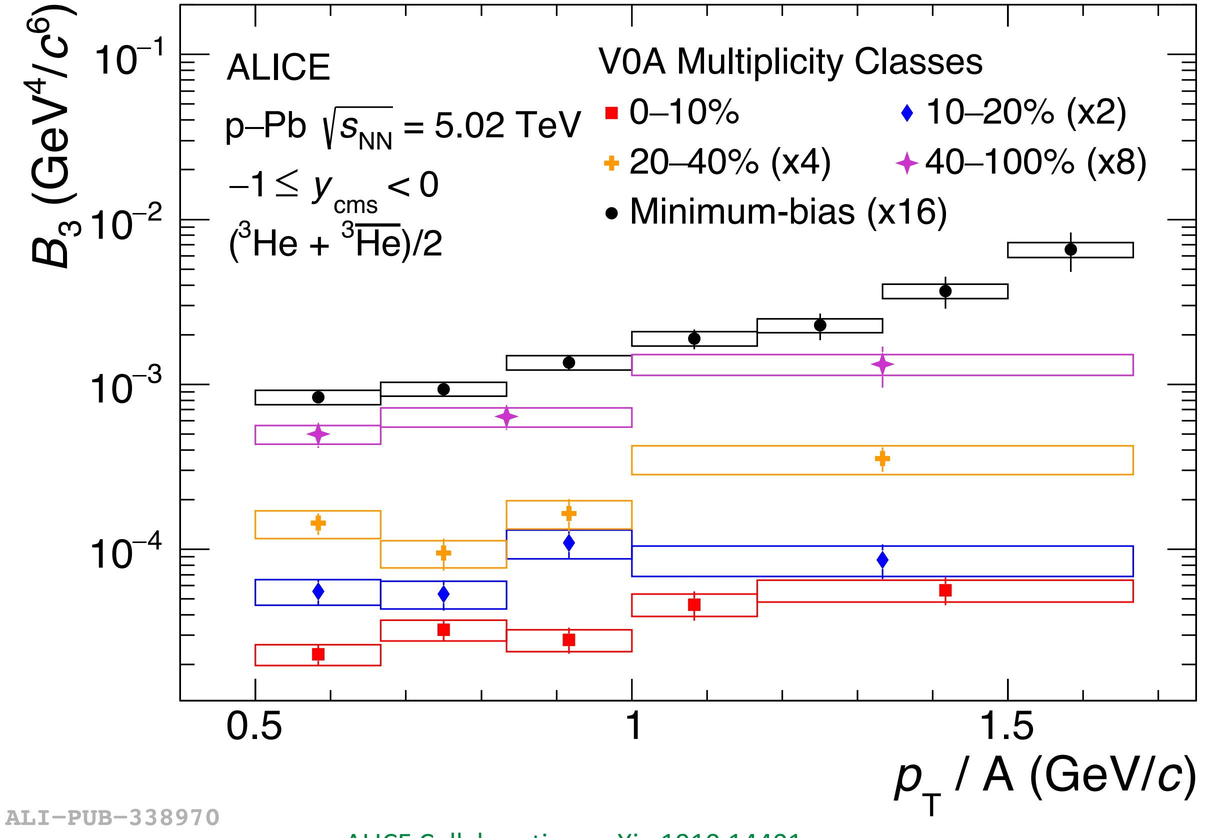

ALICE Collaboration, arXiv:1910.14401

Multiplicity dependence of B_3

- B_3 shows an evolution with multiplicity, regardless of the collision system
  → Production mechanism depends only on the system size
- At lower multiplicities a flat behavior is observed
  → System size smaller than nucleus
- At higher multiplicities a decreasing trend is observed
  → System size larger than nucleus

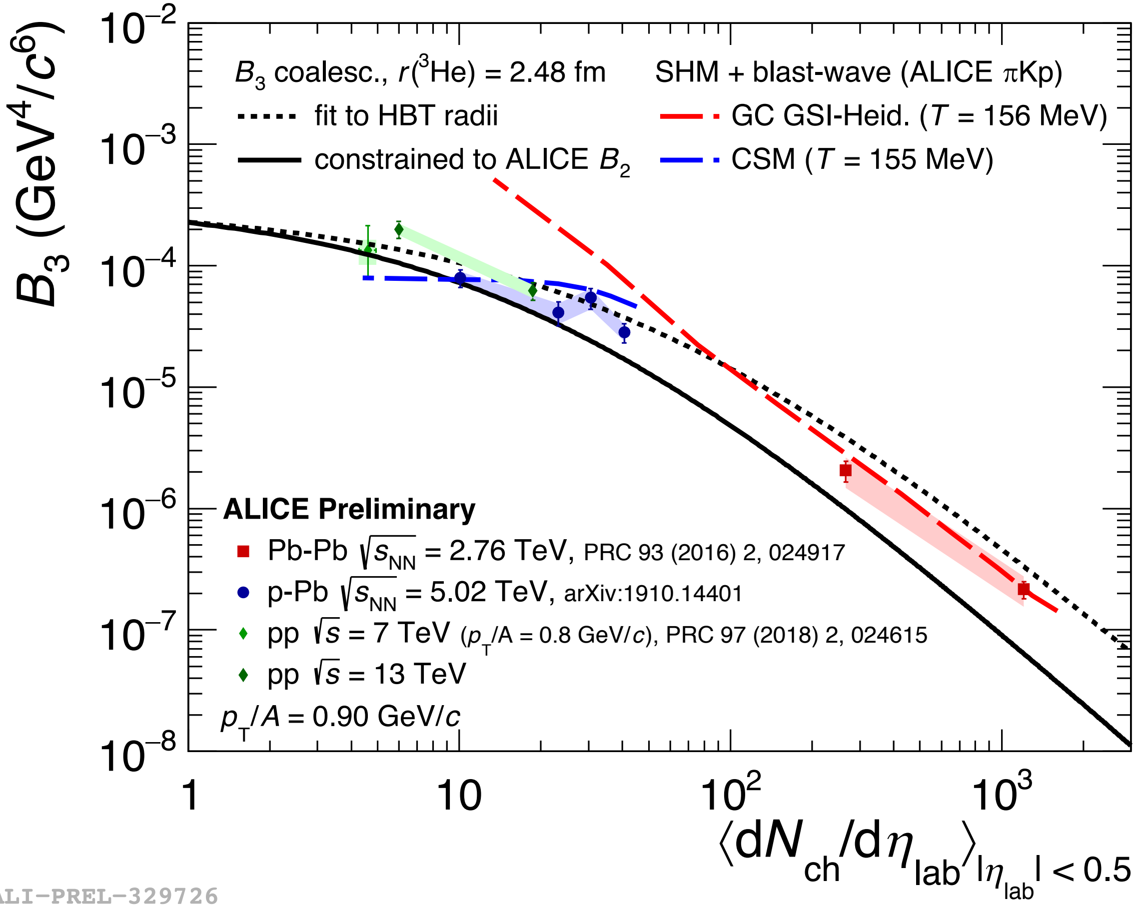

Multiplicity dependence of B_2

- B_2 shows an evolution with multiplicity, regardless of the collision system
  → Production mechanism depends only on the system size
- At lower multiplicities a flat behavior is observed
  → System size smaller than deuteron
- At higher multiplicities a decreasing trend is observed
  → System size larger than deuteron

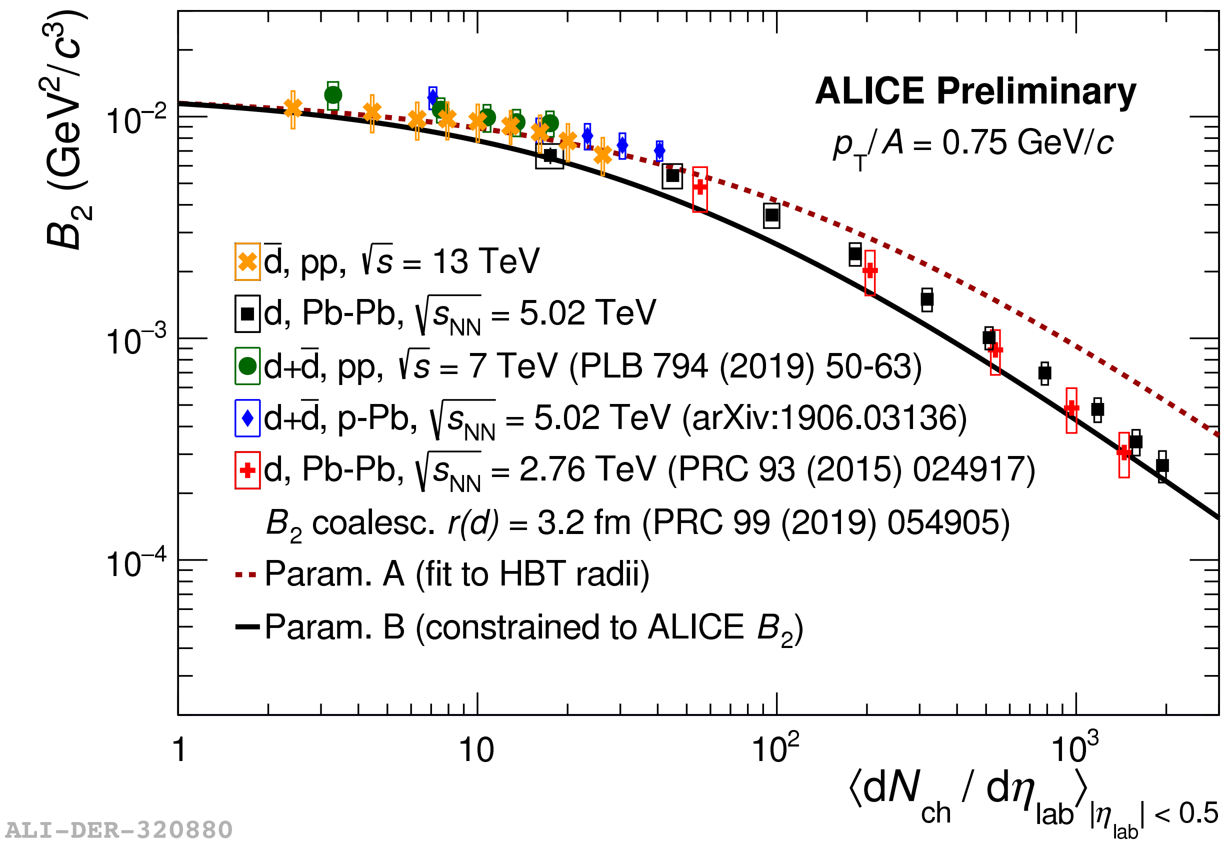

Deuteron over proton ratio versus multiplicity

- Ratio of integrated yield of A=2 nuclei (deuterons) over integrated proton yield shows a clear trend as function of multiplicity measured in different collision systems
- Increasing trend from pp to p-Pb and saturation in Pb-Pb rather well described by thermal and coalescence models

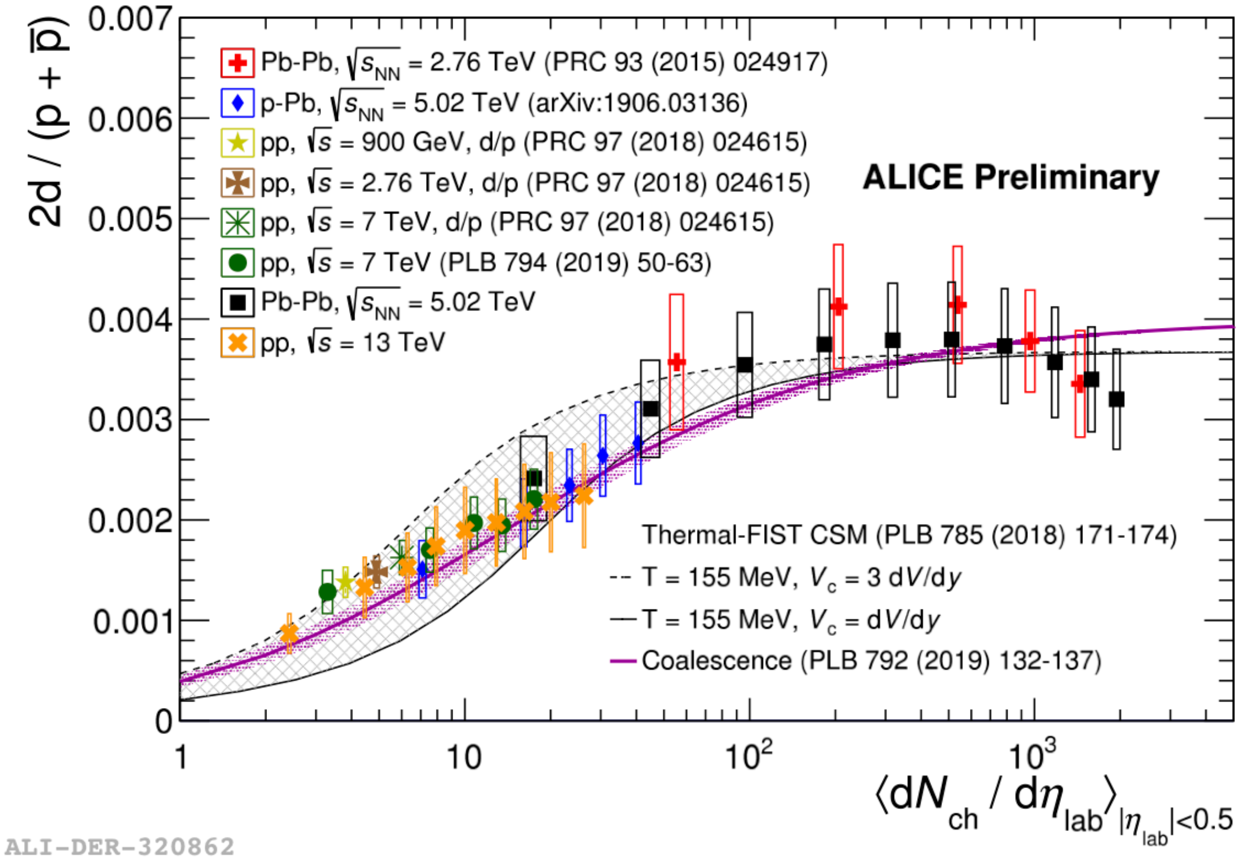

^{3}He and triton over proton versus multiplicity

2018 high-statistics data set

- Ratio of integrated yield of A=3 nuclei over integrated proton yield shows a clear trend as function of multiplicity measured in different collision systems
- Increasing trend from pp to p-Pb and saturation in Pb-Pb rather well described by thermal and coalescence models

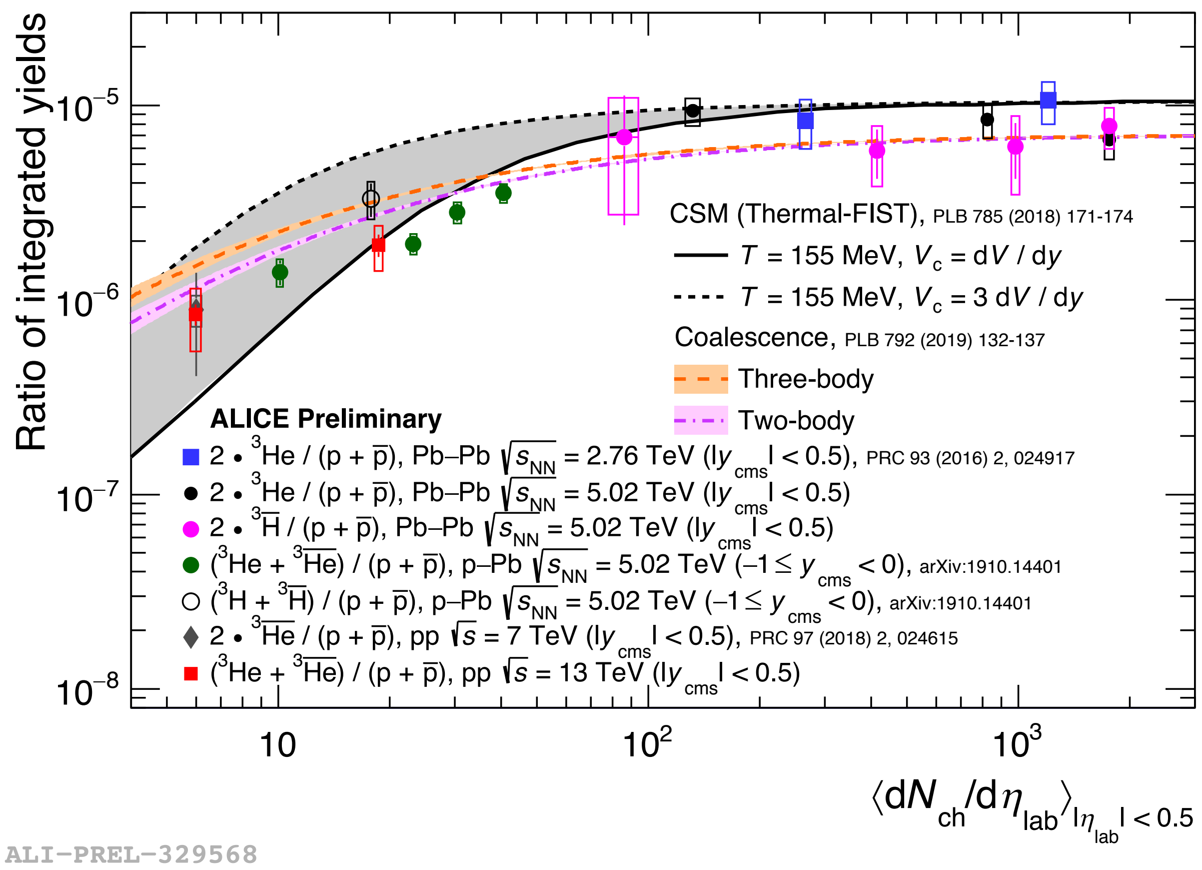

Hypertriton lifetime

Hypertriton

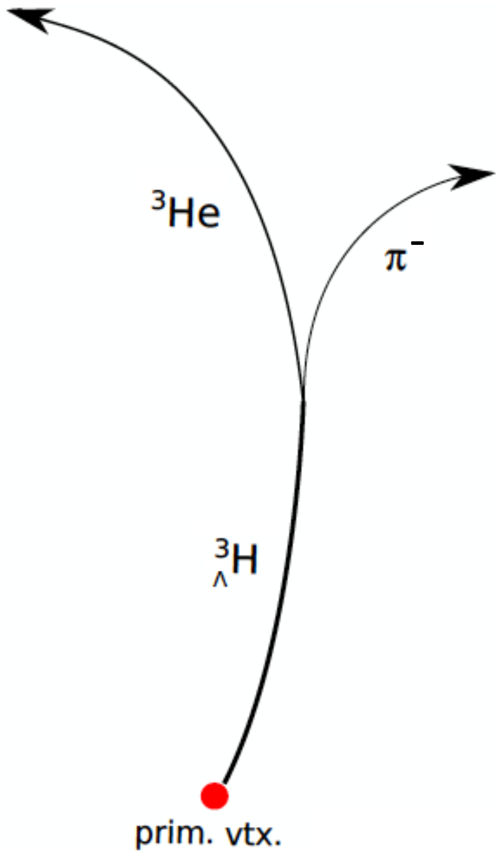

- Bound state of Λ, p and n
- m = 2.991 GeV/c^2, B_Λ = 130 keV
  → rms-radius = 10.6 fm
- Decay modes: $^3_\Lambda\mathrm{H} \rightarrow {}^3\mathrm{He} + \pi^-$

  $^3_\Lambda\mathrm{H} \rightarrow {}^3\mathrm{H} + \pi^0$

  $^3_\Lambda\mathrm{H} \rightarrow \mathrm{d} + \mathrm{p} + \pi^-$

  $^3_\Lambda\mathrm{H} \rightarrow \mathrm{d} + \mathrm{n} + \pi^0$

  + anti-particles

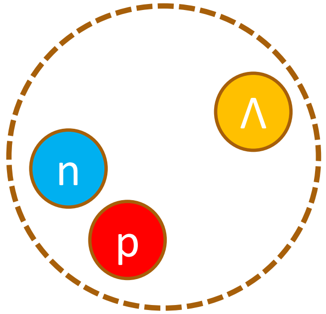

Hypertriton

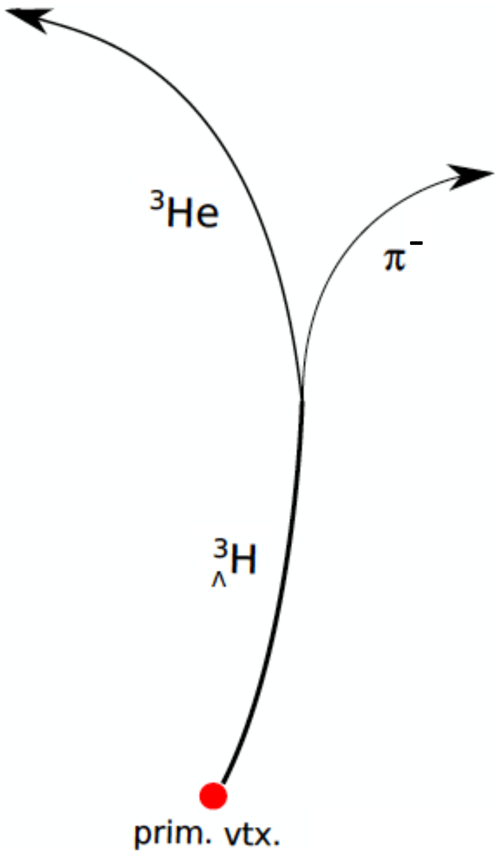

- Bound state of Λ, p and n
- m = 2.991 GeV/c^2, B_Λ = 130 keV
  → rms-radius = 10.6 fm
- Decay modes: $^3_\Lambda\mathrm{H} \rightarrow {}^3\mathrm{He} + \pi^-$

$$^3_\Lambda\mathrm{H} \rightarrow {}^3\mathrm{H} + \pi^0$$
$$^3_\Lambda\mathrm{H} \rightarrow \mathrm{d} + \mathrm{p} + \pi^-$$
$$^3_\Lambda\mathrm{H} \rightarrow \mathrm{d} + \mathrm{n} + \pi^0$$

\+ anti-particles

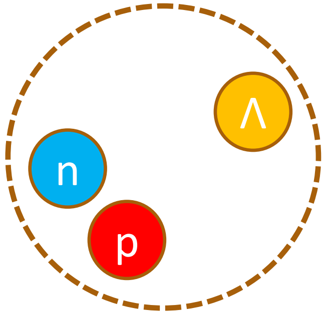

Hypertriton lifetime "puzzle"

- Data before 2010 coming from emulsion and bubble chamber experiments
- Most precise measurements coming from heavy-ion collisions
- ALICE measurement from 2015 Pb-Pb data set (red) just published
  → Consistent with free Λ lifetime and world average

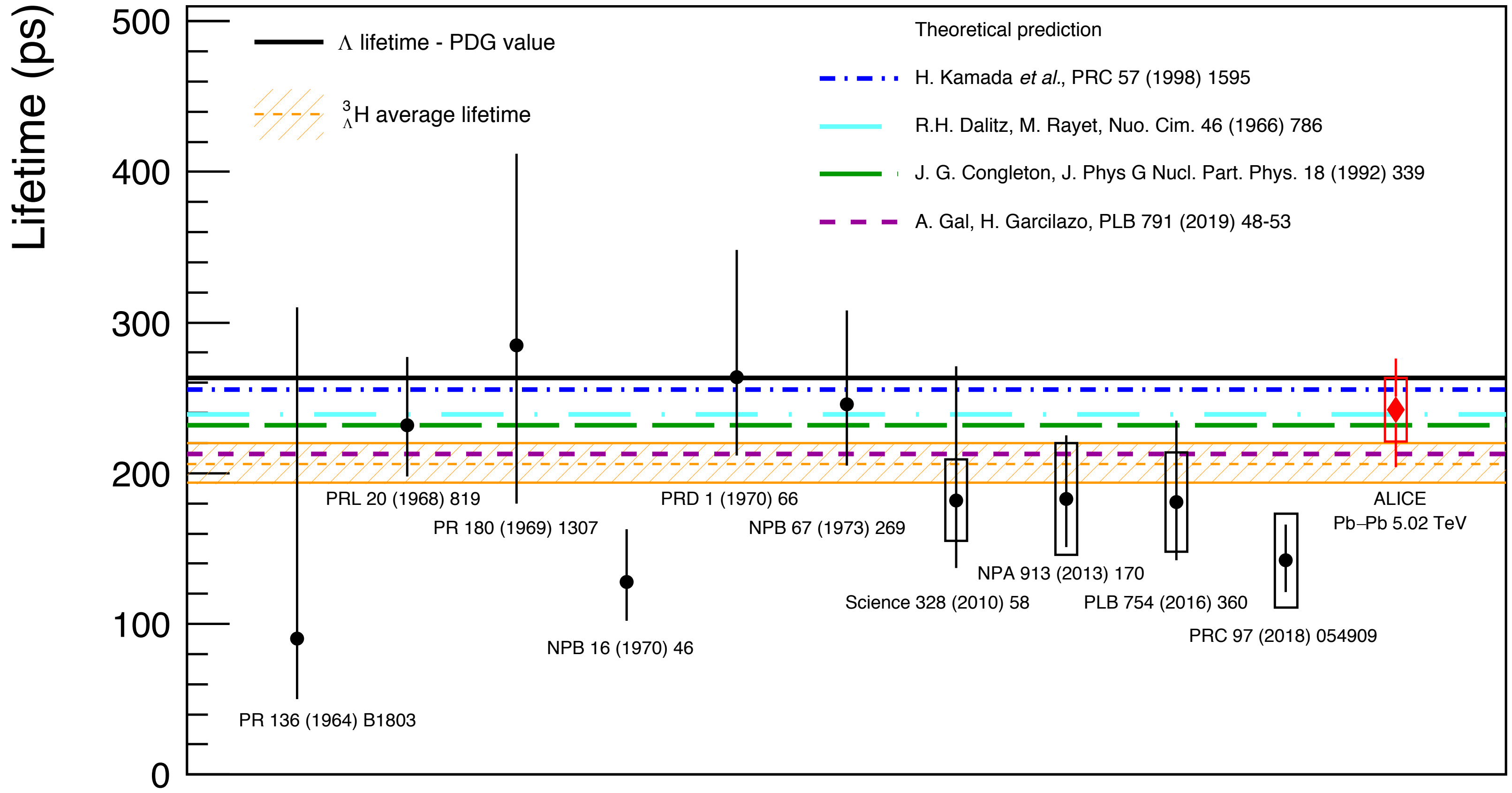

ALICE Collaboration, Phys Lett. B797 (2019) 134905

Hypertriton signal

2018 high-statistics data set

- Peak clearly visible with high significance
- Signal split in 9 *ct* bins

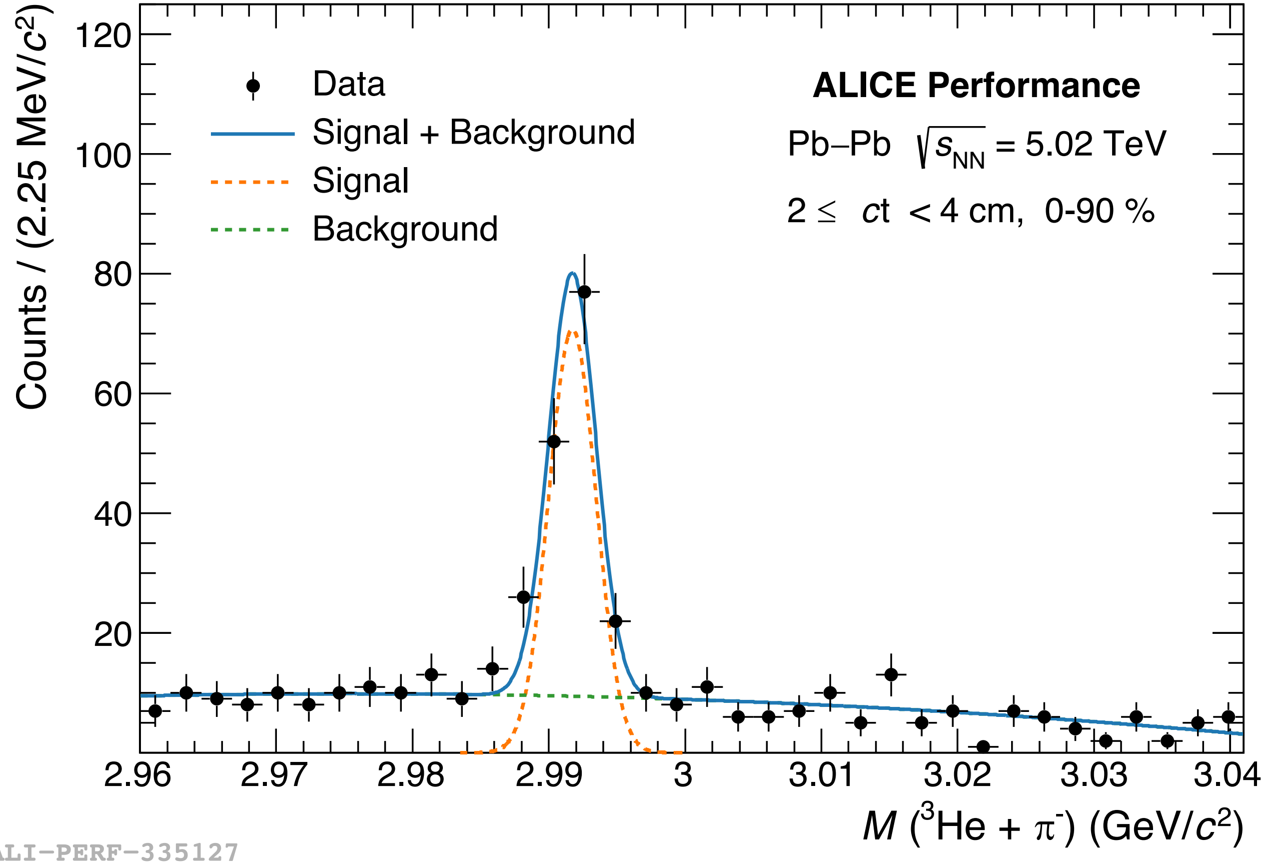

ALI-PERF-335127

Hypertriton lifetime

2018 high-statistics data set

- Peak clearly visible with high significance
- Signal split in 9 *ct* bins
- *ct* spectrum of (anti-)hypertriton with statistical and systematic uncertainties and exponential fit

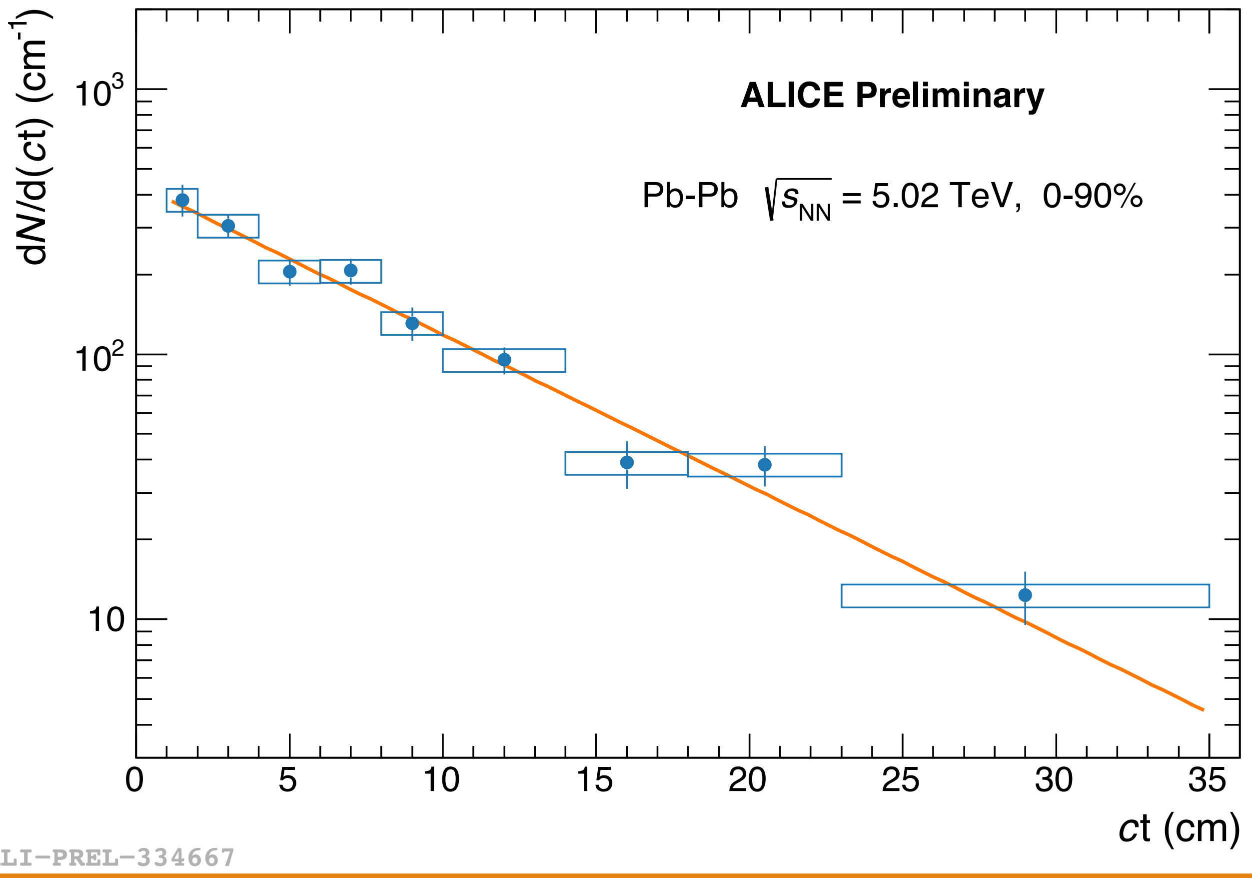

Hypertriton lifetime "puzzle"

2018 high-statistics data set

- Latest ALICE measurement (red) is most precise determination of hypertriton lifetime so far
- Consistent with free Λ lifetime and world average

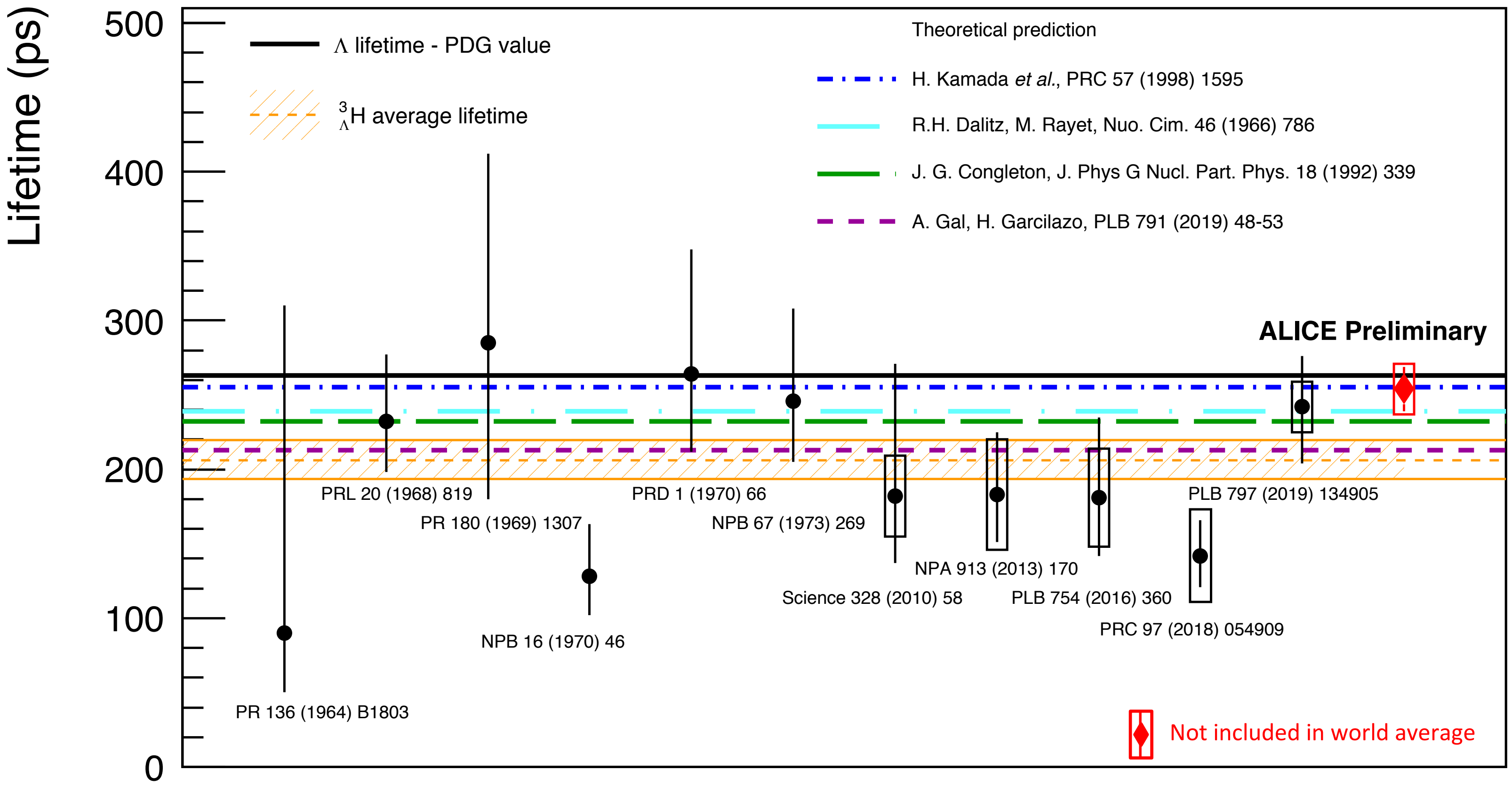

ALI−PREL−342050

Summary

- Light nuclei production in pp, p-Pb and Pb-Pb presented
- Light nuclei show significant radial and elliptic flow in Pb-Pb
- Production yields in Pb-Pb well described by the thermal model
- Coalescence parameters B_2, B_3 and particle yield ratios show common trend with multiplicity, well described by statistical and coalescence model
- Most precise determination of the hypertriton lifetime so far

Backup

Combined Blast-Wave fits

2018 high-statistics data set

- Simultaneous Blast-Wave fit of $\pi^{\pm}$, $K^{\pm}$, p, d, $\bar{t}$, ^{3}He and $^{4}\overline{He}$ spectra in central Pb-Pb collisions describes all particles quite well

- Fit ranges:
  - $\pi^{\pm}$: 0.5-1.0 GeV/c
  - $K^{\pm}$: 0.2-1.5 GeV/c
  - p: 0.3-3 GeV/c
  - Rest: full range